Sporadic on/off switching of HTLV-1 Tax expression is crucial to maintain the whole population of virus-induced leukemic cells

AUTHOR(S):

Mahgoub, Mohamed; Yasunaga, Jun-ichirou; Iwami, Shingo; Nakaoka, Shinji; Koizumi, Yoshiki; Shimura, Kazuya; Matsuoka, Masao

CITATION:

Mahgoub, Mohamed ...[et al]. Sporadic on/off switching of HTLV-1 Tax expression is crucial to maintain the whole population of virus-induced leukemic cells. Proceedings of the National Academy of Sciences 2018, 115(6): E1269-E1278

ISSUE DATE:

2018-01-22

URL:

http://hdl.handle.net/2433/228952

Sporadic on/off switching of HTLV-1 Tax expression is crucial to maintain the whole population of virus-induced leukemic cells

Mohamed Mahgoub[a], Jun-ichirou Yasunaga[a,1], Shingo Iwami[b,c,d], Shinji Nakaoka[c,e], Yoshiki Koizumi[f], Kazuya Shimura[a], and Masao Matsuoka[a,g,1]

[a]Laboratory of Virus Control, Institute for Frontier Life and Medical Sciences, Kyoto University, Kyoto 606-8507, Japan; [b]Mathematical Biology Laboratory, Department of Biology, Faculty of Sciences, Kyushu University, Fukuoka 819-0395, Japan; [c]Precursory Research for Embryonic Science and Technology (PRESTO), Japan Science and Technology Agency, Saitama 332-0012, Japan; [d]Core Research for Evolutional Science and Technology (CREST), Japan Science and Technology Agency, Saitama 332-0012, Japan; [e]Institute of Industrial Sciences, The University of Tokyo, Tokyo 153-8505, Japan; [f]School of Medicine, College of Medical, Pharmaceutical and Health Sciences, Kanazawa University, Ishikawa 920-8640, Japan; and [g]Department of Hematology, Rheumatology and Infectious Diseases, Kumamoto University School of Medicine, Kumamoto 860-8556, Japan

Edited by Robert C. Gallo, Institute of Human Virology, University of Maryland School of Medicine, Baltimore, MD, and approved December 20, 2017 (received for review September 7, 2017)

Viruses causing chronic infection artfully manipulate infected cells to enable viral persistence in vivo under the pressure of immunity. Human T-cell leukemia virus type 1 (HTLV-1) establishes persistent infection mainly in CD4+ T cells in vivo and induces leukemia in this subset. HTLV-1–encoded Tax is a critical transactivator of viral replication and a potent oncoprotein, but its significance in pathogenesis remains obscure due to its very low level of expression in vivo. Here, we show that Tax is expressed in a minor fraction of leukemic cells at any given time, and importantly, its expression spontaneously switches between on and off states. Live cell imaging revealed that the average duration of one episode of Tax expression is ∼19 hours. Knockdown of Tax rapidly induced apoptosis in most cells, indicating that Tax is critical for maintaining the population, even if its short-term expression is limited to a small subpopulation. Single-cell analysis and computational simulation suggest that transient Tax expression triggers antiapoptotic machinery, and this effect continues even after Tax expression is diminished; this activation of the antiapoptotic machinery is the critical event for maintaining the population. In addition, Tax is induced by various cytotoxic stresses and also promotes HTLV-1 replication. Thus, it seems that Tax protects infected cells from apoptosis and increases the chance of viral transmission at a critical moment. Keeping the expression of Tax minimal but inducible on demand is, therefore, a fundamental strategy of HTLV-1 to promote persistent infection and leukemogenesis.

HTLV-1 | Tax | HBZ | adult T-cell leukemia–lymphoma | computational simulation

Chronic viral infection is established when there is a metastable balance between host immunity and viral strategies for maintaining infected cells in infected individuals. Several human viruses cause persistent infection and are closely associated with inflammatory diseases and/or cancers (1). Human T-cell leukemia virus type 1 (HTLV-1) and human herpesviruses (HHVs), such as EBV (HHV-4) and Kaposi's sarcoma-associated virus (KSHV; HHV-8), are representatives of this type of virus (2) and express a limited number/amount of viral products, enabling infected cells to survive in vivo by escaping from host immune surveillance. Reactivation of viral replication, such as in the lytic phase of EBV and KSHV infection, is then a critical step for facilitating viral transmission to new hosts. Human oncogenic viruses encode the regulatory factors, which are involved in viral replication and cellular oncogenesis (3); however, their expression dynamics and the roles in each phase are poorly understood.

HTLV-1 is a human retrovirus that chronically infects CD4+ T cells. Some infected individuals develop a malignant disease of CD4+CD25+ T cells, adult T-cell leukemia–lymphoma (ATL), and/or inflammatory diseases, such as HTLV-1–associated myelopathy/tropical spastic paraparesis and HTLV-1 uveitis (4, 5). Unlike that of HIV, the replication of HTLV-1 is at a very low level in vivo, and viral RNA is rarely detected in the plasma of infected individuals (6). Instead, this virus persists in the host by using two different strategies: cell-to-cell transmission of viral particles (de novo infection) and clonal proliferation of infected cells (mitotic expansion) (7, 8).

HTLV-1 encodes two oncogenic factors, Tax and human T-cell leukemia virus type 1 bZIP factor (HBZ), in the sense and antisense strands of provirus, respectively, and these two factors counteract each other in many signaling pathways (9). Tax is not only a potent oncoprotein (10) but also an efficient transactivator of viral replication, which means that Tax is required for de novo infection. However, Tax expression is generally suppressed in infected cells in vivo (11). In contrast, HBZ is constitutively expressed in infected cells and plays important roles in viral latency (8) and

Significance

The oncogenic retrovirus human T-cell leukemia virus type 1 (HTLV-1) encodes Tax, an activator of both viral replication and cellular oncogenic pathways. Despite the potent activities of Tax, its precise roles in pathogenesis remain unclear, since it is faintly expressed in vivo. This study shows that sporadic and transient Tax expression is observed in a small subpopulation of HTLV-1–induced leukemic cells. This limited Tax expression is critical for survival of the whole population through ignition of antiapoptotic signals. Tax is induced by various stresses, suggesting that Tax efficiently protects cells from apoptosis and reactivates virus from reservoirs under conditions of cellular stress. It is an elaborated strategy of HTLV-1 to evade host immunity and enable persistence in vivo.

Author contributions: M. Mahgoub, J.-i.Y. and M. Matsuoka designed research; M. Mahgoub, J.-i.Y., S.I., S.N., K.S., and M. Matsuoka performed research; M. Mahgoub, J.-i.Y., S.I., S.N., Y.K., K.S., and M. Matsuoka analyzed data; and M. Mahgoub, J.-i.Y., S.I., S.N., and M. Matsuoka wrote the paper.

The authors declare no conflict of interest.

This article is a PNAS Direct Submission.

Data deposition: The RNA-Seq data reported in this paper have been deposited in the Gene Expression Omnibus (GEO) database, https://www.ncbi.nlm.nih.gov/geo (accession no. GSE108601). C++ source code is freely available at https://github.com/petadimension/Tax_dynamics/. R source code is available at https://github.com/petadimension/Tax_dynamics/tree/master/ABM.

[1]To whom correspondence may be addressed. Email: jyasunag@infront.kyoto-u.ac.jp or mamatsu@kumamoto-u.ac.jp.

This article contains supporting information online at www.pnas.org/lookup/suppl/doi:10.1073/pnas.1715724115/-/DCSupplemental.

proliferation of infected cells (12). These facts suggest that HTLV-1 fine-tunes the expression and function of these counteracting viral factors to establish persistent infection in infected individuals. Since Tax is highly immunogenic (13–15), HTLV-1 seems to minimize Tax expression to escape from host immunity. Therefore, the significance of Tax in leukemogenesis has been an important unsolved issue.

In this study, we show that only a small fraction (0.05–3%) of cells transiently expresses Tax. However, knockdown (KD) of Tax induced apoptosis in the majority of cells, suggesting that Tax expressed in a minor subset is required for survival of the whole population. At a single-cell level, Tax-expressing cells highly expressed several antiapoptotic and NF-κB–related genes, and Tax-negative cells were divided into two subpopulations, which expressed medium or low levels of the antiapoptotic genes. Computational simulations support our hypothesis that transient Tax expression confers an antiapoptotic property on the expressing cell and that this effect lasts after Tax expression is diminished. This study shows the dynamics of Tax expression at a single-cell level and shows roles of Tax in establishing persistent infection by HTLV-1.

Results

A Small Fraction of MT-1 Cells Expresses Tax, and This Expression Is Critical for the Survival of the Whole Cell Population. HTLV-1 *tax* is generally silenced or transcribed at quite low levels in ATL cells in vivo (16). An ATL cell line, MT-1, has an equivalent expression profile of viral genes to primary HTLV-1–infected cells (17). We carried out single-cell qRT-PCR to elucidate the expression levels of *tax* and *HBZ* in individual MT-1 cells. The initial experiment showed that only 1 in 71 cells expressed a high level of *tax*, while no detectable expression was observed in the remaining 70 cells (Fig. 1*A*). In contrast, *HBZ* was expressed in Tax-negative cells, while it was not detected in the Tax-expressing cell. These results suggest that the expression of *tax* and *HBZ* is strictly and reciprocally regulated in MT-1 cells.

Our next question was the following: what is the role of Tax expression in a small number of MT-1 cells? To address this issue, we knocked down Tax with shRNA. Two different lentivirus vectors expressing shRNA targeting Tax (shTax1 and shTax4) were transduced into MT-1 cells, and each construct efficiently inhibited Tax expression to ∼15% of the level in control cells (Fig. 1*B*, *Left*). Intriguingly, progressive cell death was observed in MT-1 cells after Tax was knocked down (Fig. 1*B*, *Right*), and as a mechanism, we found that Tax-KD induced apoptosis of MT-1 cells but not Jurkat cells (Fig. 1*C* and Fig. S1). To compare population dynamics between Tax-KD cells and Tax-intact cells, a GFP competition assay was carried out (schema in Fig. 1*D*, *Left*). To our surprise, ∼90% of shTax-transduced cells were eliminated from culture by day 21 (Fig. 1*D*, *Right*), which was faster than we expected. These results indicated that Tax is indispensable for the survival of MT-1 cells, although only a small fraction of MT-1 cells expresses it. Since shTax-transduced cells were not rescued by the presence of nontransduced cells, it also seems that a cell's survival may depend at least partly on Tax expression within that cell rather than depending on Tax expression by neighboring cells.

Tax Is Transiently Expressed in MT-1 Cells. We wished to further distinguish between these two possible hypotheses: (*i*) that a small population of cells constantly expresses Tax and supports the survival of the whole population or (*ii*) that all cells transiently express Tax by turns. To monitor Tax expression, we established a reporter subline of MT-1, MT1GFP, which expresses destabilized EGFP (d2EGFP; the half-life of the modified EGFP is 2 h) under the control of 18 copies of the Tax-responsive element (schema in Fig. 1*E*, *Upper*) (18). It was confirmed that d2EGFP expression in MT1GFP cells was closely correlated with Tax expression by intracellular staining with anti-Tax antibody, and a very small population (∼0.5%) of MT1GFP cells expressed d2EGFP (plot in Fig. 1*E*, *Lower*). Several stable clones of MT1GFP were established, and all clones possessed a small Tax-expressing subset. Using one of the MT1GFP clones, we evaluated the dynamics of Tax expression in individual cells by time-lapse imaging. The result revealed that d2EGFP expression was transient in most d2EGFP-positive cells (Fig. 1*F* and Movie S1), indicating that Tax is expressed temporarily in MT-1 cells. We could also see cells with fluctuating and continuous patterns of d2EGFP expression (Fig. 1*G* has definitions of these terms), although the percentages of cells with those patterns were lower than cells with transient expression (6% for fluctuating and 18% for continuous cells) (Fig. 1*G*). Analysis of 87 cells with transient d2EGFP expression showed that the median and mean durations of Tax expression were ∼22 and 18 h, respectively (95% confidence interval, 19.3–24.7) (Fig. 1*H*).

It has been reported that two other ATL cell lines, KK-1 and SO-4, have expression levels of Tax and HBZ similar to those of fresh ATL cells (17). Small fractions of KK-1 and SO-4 cells each expressed Tax, and a subline of KK-1 reporting Tax expression, KK1GFP, was successfully established (Fig. S2 *A* and *B*). Since DNA hypermethylation in 5′ LTR is known to suppress *tax* transcription, we evaluated its methylation level and *tax* expression in fresh ATL cells and three ATL cell lines (MT-1, KK-1, and SO-4). In approximately one-half of ATL cases and all cell lines, DNA methylation level of 5′ LTR was low, and *tax* mRNA was detectable, suggesting that *tax* expression is inducible in these cells (Fig. S2*C*).

Computer Simulation Represents the Dynamics of Tax Expression. It was an incomprehensible observation that KD of Tax in a minor fraction (∼0.5%) of MT-1 cells induced progressive apoptosis. To estimate the duration that all MT-1 cells experience Tax expression, we used a computational simulation based on a mathematical model. A previous study on HIV elegantly established a mathematical model of 5′ LTR activation by Tat in latently infected cells (19). We adapted this model to simulate the regulation of the HTLV-1 5′ LTR by Tax (details are in *SI Materials and Methods*, and Fig. S3*A* shows a schematic representation). We tested several parameters used in the HIV study and adjusted them to fit our experimental data of transient Tax expression (*SI Materials and Methods*, Fig. S3 *B–D*, and Table S1). The simulation could then successfully reproduce the dynamics of Tax expression in MT-1 cells, and the calculated mean duration of Tax expression was 13.6 h, consistent with experimental observations (Fig. S3*C*), suggesting that the parameters that we used were suitable for the model for activation of the HTLV-1 LTR. Using this model, we then estimated the distribution of the interval between two successive Tax expression episodes (Fig. S3*E*), and interestingly, our simulation reproduced the single-cell level expression pattern of Tax (Fig. S3*F*). Furthermore, we calculate that it takes ∼150 d for 90% of MT-1 cells to experience Tax expression (Fig. S3*G*). This result means that the loss of Tax-KD cells occurs much faster than the Tax expression (Fig. 1*D*). The details of our single cell-level computational simulations are described in *SI Materials and Methods*.

This simulation suggests a possible mechanism that short-term expression of Tax by a cell confers some effects on not only to the cell during its period of Tax expression but also, to the cell and its progeny, even after Tax expression is lost.

Distinct Transcriptional Profiles in Tax-Expressing Cells. To clarify the effects of Tax on both Tax-expressing cells and nonexpressing cells, we analyzed the transcriptional profiles of each population. Tax-expressing MT1GFP or KK1GFP cells (Fig. 1*E* or Fig. S2*B*, respectively) were purified from bulk cells by a cell sorter using d2EGFP as a marker for Tax, and RNAs from each fraction were subjected to RNA-Seq. Many T-cell activation-associated genes were differentially regulated in Tax-expressing cells compared

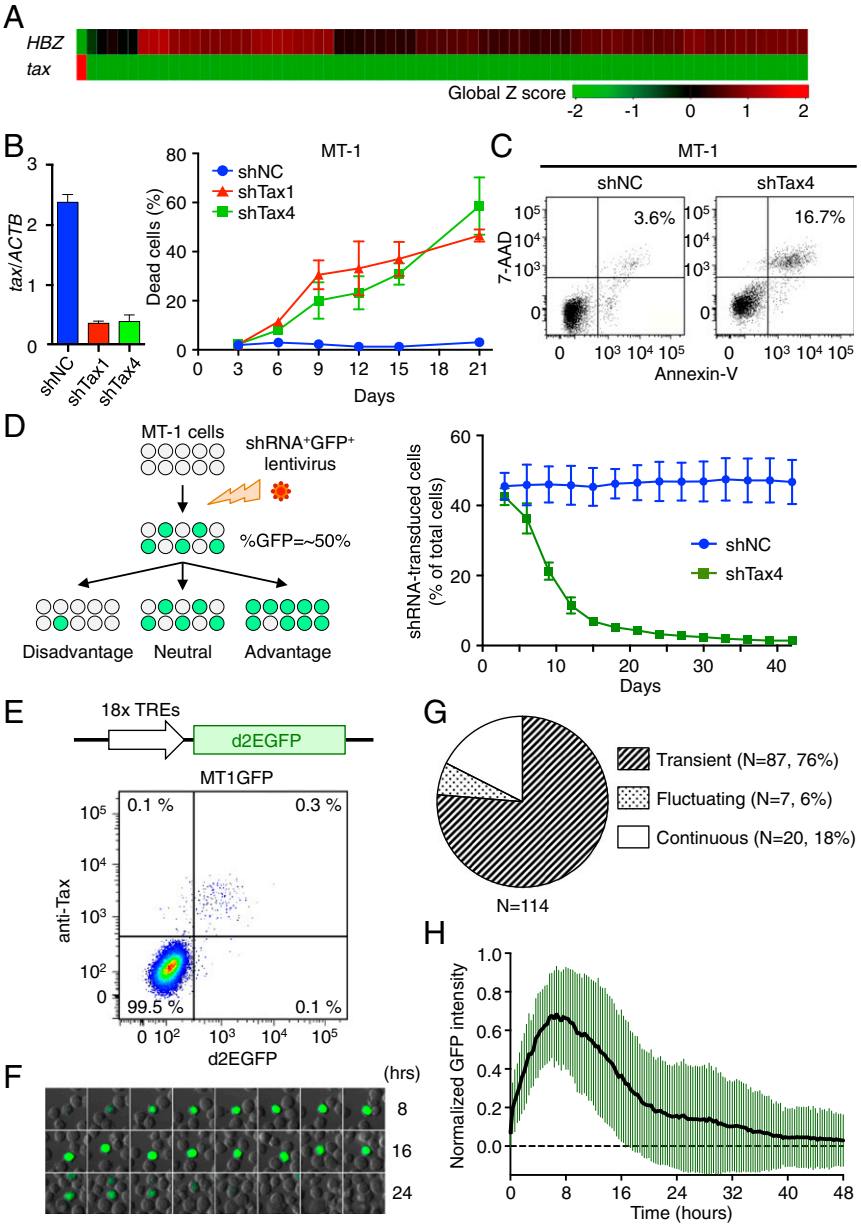

Fig. 1. Significance and dynamics of Tax expression at a single-cell level in MT-1 cells. (*A*) Single-cell qPCR for *tax* and *HBZ* expression in MT-1 cells ($n = 71$). (*B*, *Left*) Efficiency of Tax-KD by shRNA. (*B*, *Right*) The percentage of cells that are dead after Tax-KD. MT-1 cells were infected with a bicistronic lentivirus vector expressing GFP and shRNA (shTax1, shTax4, or shNC). Cells were stained with LIVE/DEAD reagent, and the ratio of dead cells to shRNA-transduced (GFP+) cells was measured by flow cytometry. (*C*) AnnexinV/7-AAD double staining in shRNA-transduced MT-1 cells at day 15 posttransduction. (*D*, *Left*) Schematic depicting the concept behind the GFP competition assay. The ratio of GFP+ cells changes over time depending on the effect of shRNA on transduced cells. (*D*, *Right*) Serial measurements of the percentage of GFP+ cells among the whole MT-1 cell population after shNC or shTax4 transduction. For *B* and *D*, error bars show SDs for three experiments. (*E*, *Upper*) Scheme of Tax reporter cassette that expresses d2EGFP. MT1GFP is a stable subline of MT-1 transduced with this cassette. (*E*, *Lower*) Intracellular Tax staining of MT1GFP. (*F*) Live cell imaging of Tax expression in MT1GFP cells. This montage of time-lapse images shows changes in d2EGFP expression. (*G*) Expression pattern of Tax in MT1GFP. Cells were categorized based on their pattern of d2EGFP expression during the observation period. Continuous, cell continuously expressed d2EGFP until the end of observation period; fluctuating, cell has multiple episodes; transient, cell has a single spontaneous episode. (*H*) Single-cell dynamics of d2EGFP expression for 87 cells with transient expression. Mean ± SD is shown.

with nonexpressing cells (Fig. 2 *A* and *B*). Upstream regulator analysis was carried out using the Ingenuity Pathway Analysis program and revealed that NF-κB–related pathways were significantly affected by Tax in both cell lines (Fig. 2*B*).

To analyze the correlation between Tax expression and that of other genes at a single-cell level, we chose ∼90 representative genes in addition to *HBZ* and compared their mRNA levels in sorted Tax-positive vs. Tax-negative MT-1 cells by single-cell qRT-PCR. As expected, clustering analysis could clearly separate Tax-positive cells from Tax-negative cells (Fig. 2*C*). Expression of NF-κB target genes and apoptosis-related genes was positively correlated with that of *tax* in each MT-1 cell (Fig. 2*D* and Fig. S4). Interestingly, violin plots of several antiapoptotic genes, such as *CFLAR*, *GADD45B*, *TRAF1*, and *TNFAIP3*, showed two peaks in Tax-negative cells: one with almost no expression and another with lower expression than Tax-positive cells (Fig. 2*D*). In addition, a 3D principal component analysis (PCA) plot generated by the expression levels of these genes revealed that there were two clusters in Tax-negative cells (Fig. 2*E*). These findings suggest that Tax influences the expression of antiapoptotic genes in Tax-negative cells: there are two subpopulations—those with medium and those with low levels of antiapoptotic factors—and thus, different degrees of sensitivity to apoptosis.

Tax Expression Is Induced by Cytotoxic Stresses and Contributes an Antiapoptotic Property to Cells. Since Tax expression was associated with the up-regulation of antiapoptotic genes, we hypothesized that Tax might be induced in response to cytotoxic stress. First, we evaluated the effect of the phases of cell growth on Tax expression. As shown in Fig. 3*A*, the percentage of d2EGFP-positive (Tax-expressing) cells increased stepwise from 1.2% at day 1 to 11.5% at day 7 if cells were cultured without passage. In contrast, the ratio of d2EGFP-expressing cells remained less than 3% when cells were properly passed, suggesting that stresses associated with the cell overgrowth triggered Tax expression. Importantly, under stressed conditions, the viability of Tax-expressing (d2EGFP+) cells was strikingly higher than that

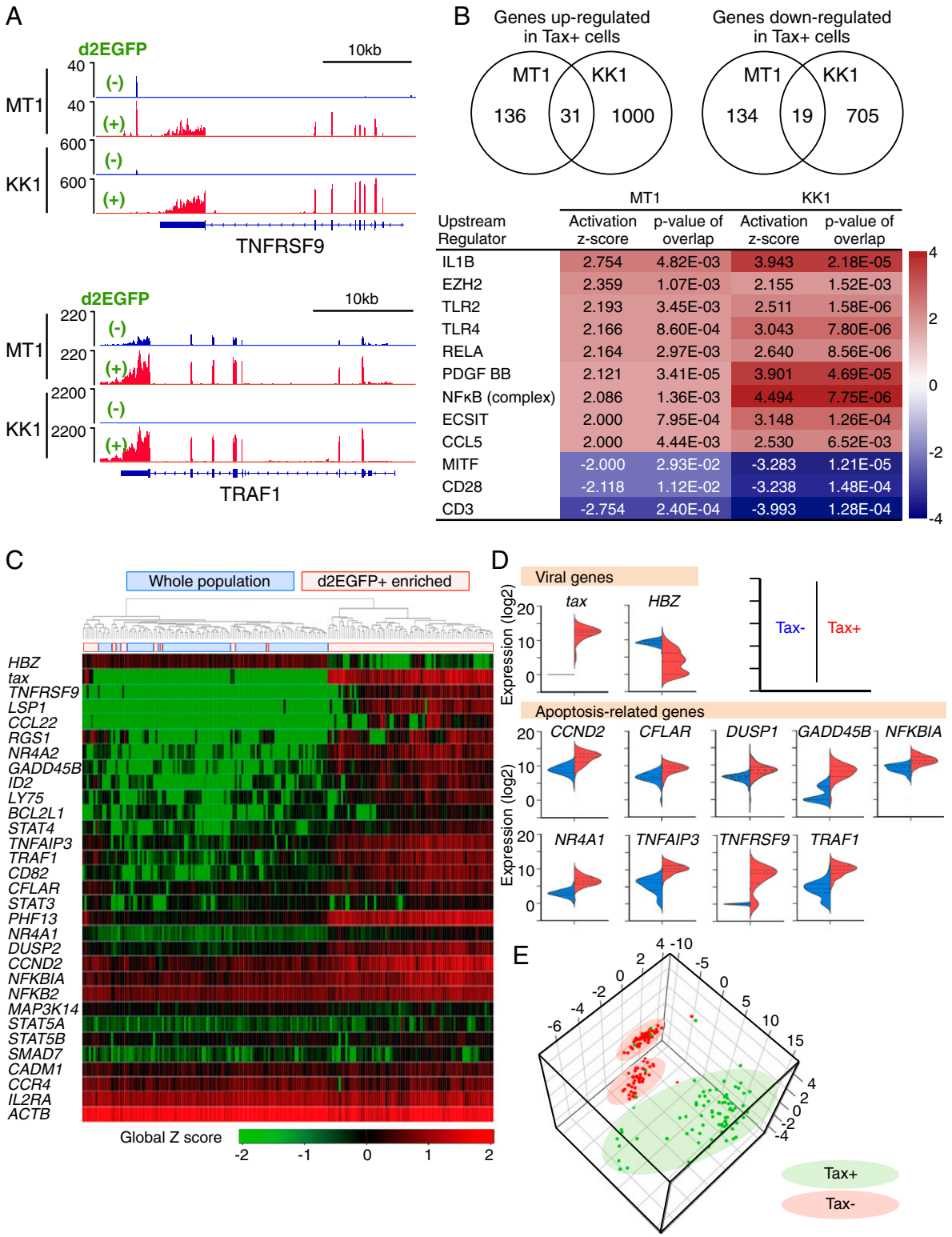

Fig. 2. Differences in gene expression between Tax-expressing and -nonexpressing MT1GFP cells. (*A*) RNA-Seq analysis comparing Tax+ and Tax− MT1GFP and KK1GFP cells. Read coverage plots for two Tax-associated genes: TNFRSF9 (*Upper*) and TRAF1 (*Lower*). (*B*) Ingenuity pathway analysis for dysregulated genes. Inclusion criteria are fragments per kilobase of transcript per million mapped reads (FPKM) ≥ 1 and greater than or equal to twofold expression change. (*Upper*) The number of dysregulated genes common to both MT1GFP and KK1GFP. (*Lower*) Top-scoring activated or inactivated upstream regulators. (*C*) Heat map of single-cell gene expression for viral and cellular genes in single MT1GFP cells. Two experiments were performed; either d2EGFP+-enriched or -unenriched (whole) populations were subjected to single-cell analysis. Ninety-four cells from each experiment were analyzed. (*D*) Violin plots comparing expression of viral- and apoptosis-related genes in the Tax+ vs. Tax− populations. Based on the apoptotic process gene list (GO:0006915; Gene Ontology database), nine apoptosis-related genes with expression levels that were significantly correlated with that of *tax* (*r* value > 0.5 by Pearson's correlation test) were identified. (*E*) 3D PCA plot showing single-cell data clustering based on expression of apoptosis-related genes from *D*.

of Tax-negative (d2EGFP−) cells (Fig. 3*B*). These observations suggest that stress-induced Tax expression confers antiapoptotic capacities on MT-1 cells.

Similarly, an inducer of oxidative stress, H_2O_2, induced Tax (Fig. 3*C*, *Left*), and the viability of Tax-expressing cells was significantly higher than that of nonexpressing cells (Fig. 3*C*, *Right*). It has been reported that one of the platinum-containing anticancer drugs, cisplatin, induces production of reactive oxygen species (ROS) in cancer cells and contributes to cytotoxicity (20). Cisplatin induced Tax in MT1GFP cells, while an inhibitor of ROS, *N*-acetyl-L-cysteine (NAC), completely canceled its effect (Fig. 3*D*). These results suggest that Tax functions as a safeguard against apoptosis induced by various cytotoxic stresses.

Similar Mechanisms for Latency of HTLV-1 and HIV. It has been known that cytotoxic stresses, such as DNA damage and oxidative stress, activate the HIV LTR (21, 22). Several HIV reactivating reagents (disulfiram, panobinostat, SAHA, and JQ-1) could also induce Tax expression in MT1GFP cells (Fig. 3*E*). JQ-1 is an inhibitor of bromodomain-containing 4 (BRD4) and robustly reactivates HIV transcription when it is used with phorbol 12-myristate 13-acetate (PMA) and ionomycin (23). A combination of JQ-1 and PMA/ionomycin exhibited potent activity on Tax induction in MT1GFP cells (Fig. 3*F*), suggesting overlapping mechanisms for latency of HTLV-1 and HIV.

It has been reported that minimum feedback circuit between HIV Tat and the HIV 5′ LTR is sufficient to establish HIV latency (19). When a lentivirus vector expressing Tat through the HIV 5′ LTR was transduced into Jurkat cells, gene expression from the 5′ LTR was highly transactivated in most cells, while a small population of infected cells became latent (24). Since our results suggested that Tax has roles similar to Tat in latency, it was tested if the HTLV-1 LTR–Tax circuit can generate latency in T cells. We found that, in Jurkat cells expressing Tax and d2EGFP through the HTLV-1 5′ LTR (Jurkat/LTRd2EGFP Tax cells), a very small population expressed d2EGFP—just as was the case for MT1GFP cells (Fig. S5*A*, *Right*). In contrast, a similar construct containing HIV Tat and HIV LTRs induced continuous expression of Tat and d2EGFP in more than 95% of cells, while a remaining subset was dormant (Fig. S5*B*); this observation was compatible with the previous report (24). Treatment by JQ-1, PMA, and ionomycin together could activate expression of d2EGFP in all Jurkat/LTRd2EGFP Tax clones (Fig. S5*C*), and time-lapse imaging revealed transient expression

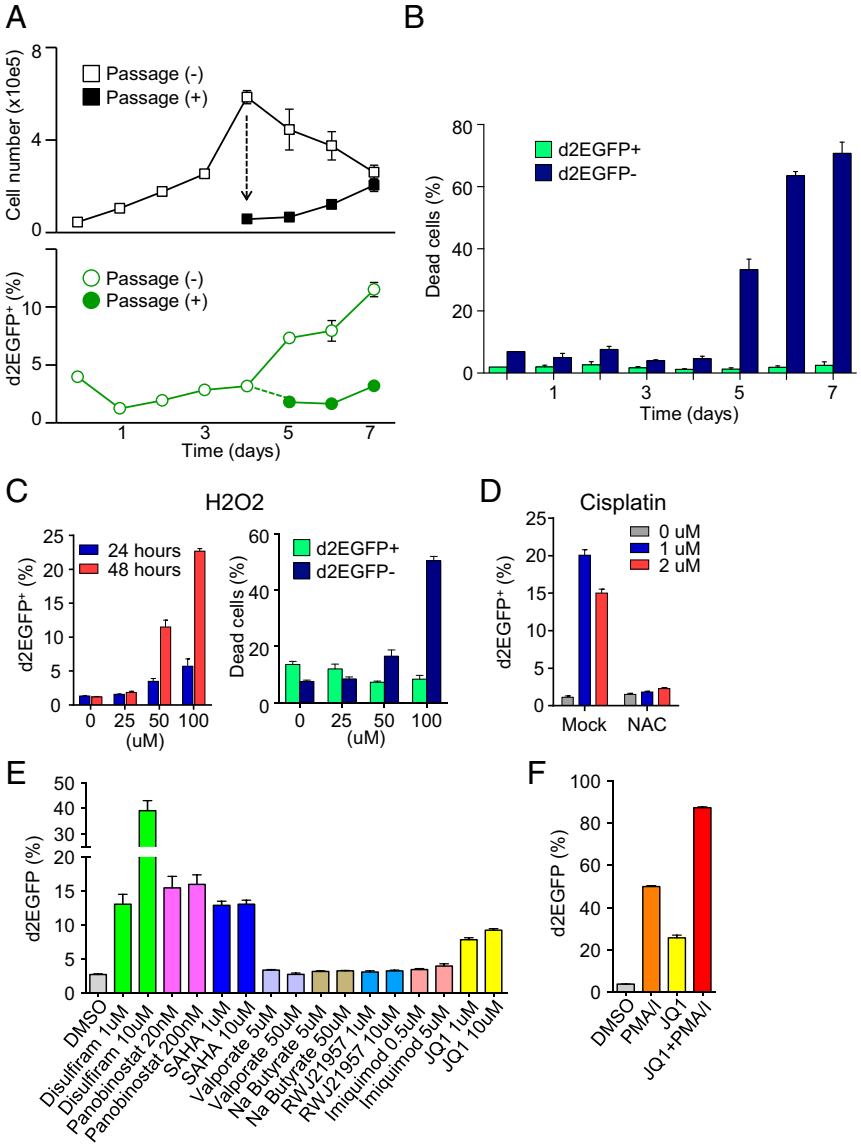

Fig. 3. Induction of Tax in MT1GFP cells by cytotoxic stresses and HIV-reactivating reagents. (*A*) Effect of cellular overgrowth on Tax expression. On day 4, cells were either passaged or allowed to overgrow. *Upper* shows cell count, and *Lower* shows percentage of cells that are d2EGFP+ (Tax+). (*B*) Effect of cellular overgrowth on cell viability in d2EGFP+ (Tax+) and d2EGFP− (Tax−) cells. Viability is measured by LIVE/DEAD staining. (*C*) Induction of Tax expression by H_2O_2 treatment. (*Left*) Percentage of cells that are d2EGFP+ (Tax+); (*Right*) viability (LIVE/DEAD staining) of d2EGFP+ (Tax+) and d2EGFP− (Tax−) cells after 48 h. (*D*) Induction of Tax expression by cisplatin treatment is reversed by the antioxidant NAC. (*E* and *F*) Effect of HIV-reactivating reagents on Tax expression in MT1GFP cells. (*E*) The effect of HIV-reactivating reagents on Tax expression. MT1GFP cells were treated for 18 h with the indicated drugs that have been previously reported to reactivate HIV expression. (*F*) The effect of a combination of JQ-1 and PMA/I on Tax expression. The percentage of cells that are d2EGFP+ was measured by flow cytometry. Each figure is a representative of two independent experiments. Error bars show SDs for three replicates in one experiment.

of d2EGFP in some untreated Jurkat/LTRd2EGFP Tax cells (Fig. S5*D*). These findings suggest that the Tax–5′ LTR circuit is a basic unit for modulating Tax expression flexibly in response to various stimulations.

Tax Suppresses the Cell Cycle Transition from S to G2/M. A possible alternate explanation for the big impact of Tax-KD on MT-1 cell survival was that Tax-expressing cells might proliferate faster than nonexpressing cells. To test this hypothesis, the effect of Tax on the cell cycle was analyzed using a method combining DAPI staining and 5-ethynyl-2′-deoxyuridine (EdU) incorporation (Fig. 4*A*)—a method by which we can evaluate temporal cell cycle progression without synchronization (25). We found that the proportions of cells in S and G2/M phases 2 h after the start of an EdU pulse were comparable between Tax-positive and Tax-negative cells. However, at 6 h, the proportion of G2/M cells within the Tax-positive population was only ∼80% of that within the Tax-negative population (G2/M cells made up 39.4 and 48.7% of Tax-positive and -negative cells, respectively), suggesting that, if anything, Tax retarded, rather than sped up, the G2/M transition of MT-1 cells (Fig. 4 *B* and *C*). This result implies that Tax does not promote faster proliferation of expressing cells; rather, the antiapoptotic property of Tax is responsible for the survival of MT-1 cells.

The Carryover of Antiapoptotic Factors into the Tax-Negative Interval Is Important for Maintaining the MT-1 Cell Population. Based on the results of the Tax-KD and single-cell analysis experiments, we hypothesized that transient Tax expression triggers antiapoptotic genes in a small number of MT-1 cells, that this effect is carried over in a significant number of these cells when they enter the Tax-negative phase, and that such carryover is critical for the survival and expansion of the cell population. To check this hypothesis, we constructed a population-level agent-based model (ABM) that can represent our experimental observations. More precisely, the ABM simulates the population dynamics of MT-1 cells transduced with shNC or shTax4 as an inhomogeneous (birth–death) Poisson process with a stage transition (Fig. 5*A* shows a schematic representation, and *SI Materials and Methods* has details). We carried out ABM simulations and confirmed that the time course of experimental data for the number and fraction of shNC and shTax4 cells was well-reproduced in Fig. 5 *B* and *C*. Based on our ABM simulations, we reconstructed the time course of the frequency of Tax-positive cells under normal conditions. As shown in Fig. 5*D*, our simulation predicted that a small number of MT-1 cells would express Tax (i.e., around 3% at the steady state). In addition, we calculated the predicted subpopulation dynamics of shNC and shTax4 cells (Fig. 5 *E* and *F*, respectively). The numbers of cells that are Tax positive and antiapoptotic gene positive (i.e., T_{on}), Tax negative and antiapoptotic gene high (i.e., $T_{off}A_{high}$), and Tax negative and antiapoptotic gene low (i.e., $T_{off}A_{low}$) are shown. Under normal conditions (Fig. 5*E*), the fraction of cells that are T_{on} remains small; however, the number of cells in each subpopulation increases, and the total cell population expands, since MT-1 cells are able to express Tax. This expression protects them from apoptosis. In fact, our simulation predicts that the major subpopulation will be $T_{off}A_{high}$, which is consistent with our detection of the expression of apoptosis-related genes in Fig. 2*D*. However, under Tax-KD conditions (Fig. 5*F*), the fraction of cells that are T_{on} decreases until there are almost none left, because there is no additional transition of cells from Tax negative to Tax positive. The collapse of the T_{on} subpopulation leads to a corresponding decrease in antiapoptotic gene expression, renders more cells susceptible to apoptosis, and decreases the degree to which the total cell population expands.

To examine whether having experienced Tax expression prolongs cell survival time, we also calculated the survival probabilities of the subpopulations of shNC cells in our ABM simulations (details are in *SI Materials and Methods*). For this

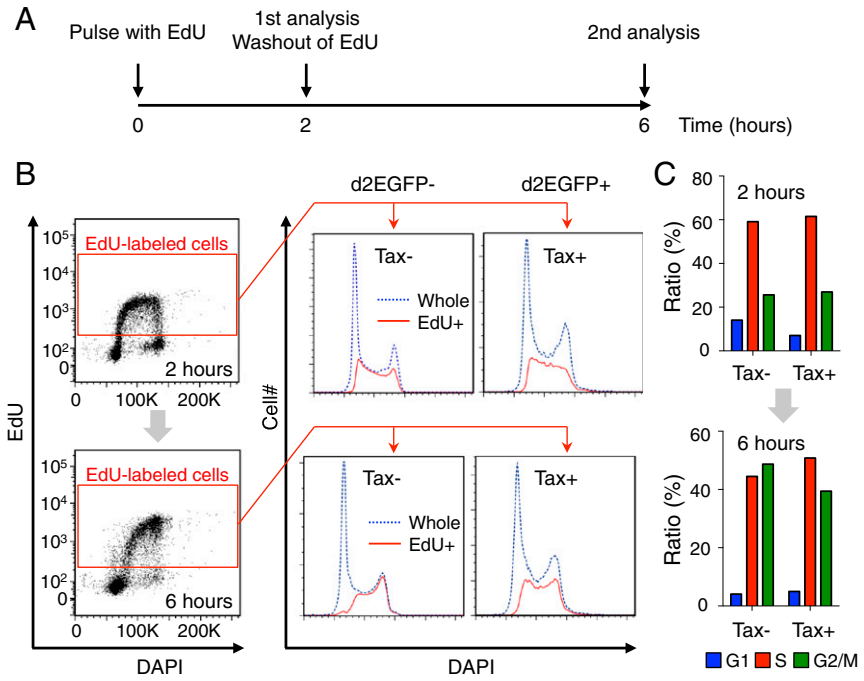

Fig. 4. Cell cycle transition in d2EGFP+ (Tax+) and d2EGFP− (Tax−) cells. (*A*) Scheme for analysis of cell cycle transition without cell synchronization. (*B* and *C*) Cell cycle phase distributions for EdU+ cells among d2EGFP+ (Tax+) and d2EGFP− (Tax−) cells at 2 and 6 h. (*B*, *Left*) Gating strategy for EdU+ cells; (*B*, *Right*) linear flow cytometric analysis of cell cycle with DAPI staining. Distribution of EdU+ cells is shown in red, and that of whole cells is blue. (*C*) Bar charts showing the percentage of EdU+ cells in the indicated phase.

calculation, we defined the subpopulations of shNC cells based on whether Tax had been expressed at least once or had never been expressed (solid and dashed lines in Fig. 5*G*, respectively). Interestingly, in this simulation, Tax expression significantly increases the average lifespan of the cell.

Taken together, these simulations support a model for ATL persistence: transient expression of Tax in cells is responsible for cell population-level maintenance and expansion (Fig. 6). In a steady state (Fig. 6, *Left*), T_{on} cells turn successively into $T_{off}A_{high}$ and then, $T_{off}A_{low}$ cells. Although $T_{off}A_{low}$ cells are sensitive to apoptotic signals and gradually die in culture, Tax-negative cells proliferate more rapidly than Tax-positive cells. In response to cytotoxic stresses, Tax can be induced in some Tax-negative cells, and thus, T_{on} cells are replenished, a process that is critical for the persistence of the population. Tax-KD (Fig. 6, *Right*) causes a decrease in T_{on} cells, resulting in a shortage of apoptosis-resistant cells and the induction of massive apoptosis. This model enables us to explain how such a small number of Tax-expressing cells has a big impact on the dynamics of the whole population.

Discussion

Persistent viruses have evolved shrewd strategies to propagate in vivo while evading host immune surveillance. Here, we show that HTLV-1 utilizes a unique way to enhance survival and proliferation of infected cells: the transient expression of Tax confers an antiapoptotic property to cells and maintains the whole population. Since it has been reported that continuous expression of Tax induces DNA damage and senescence in the expressing cells (26, 27), it is suggested that short-term expression of Tax is beneficial to cells. Interestingly, a similar phenomenon of cell survival being promoted by transient gene expression was reported in mouse ES cells (mESCs). *Zscan4*, which functions in the maintenance of telomeres, is transiently expressed in only ∼5% of mESCs at any given time. KD of *Zscan4* induces massive cell death before all cells experience its expression (28). Moreover, expression of *Zscan4* is linked to activation of an endogenous retrovirus, MERVL (29). Those studies and our observations suggest an association between the

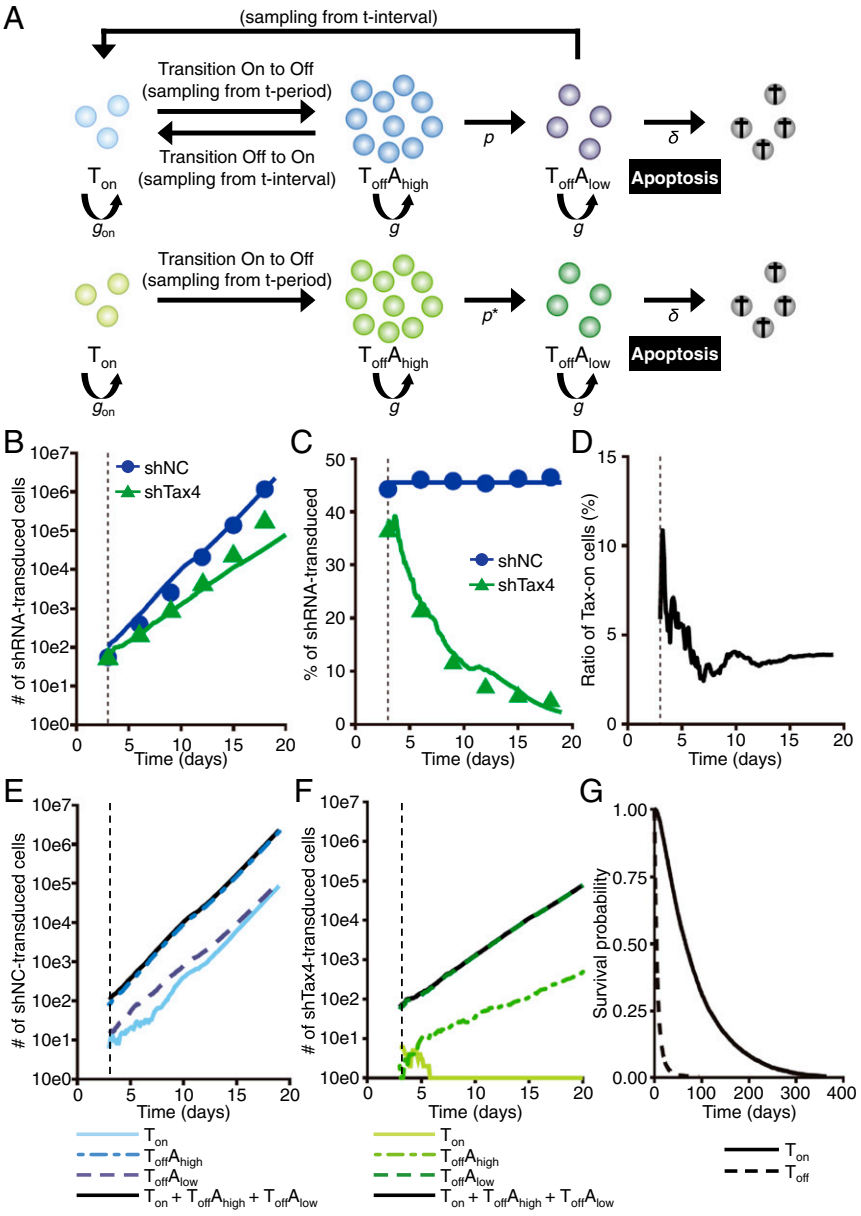

Fig. 5. Agent-based simulations of cell population dynamics under normal and Tax-KD conditions. (*A*) Scheme for modeling of cell population dynamics as a birth–death (Poisson) process with a stage transition. The ABM simulates the population dynamics of MT-1 cells transduced with shNC or shTax4. (*Upper*) Normal conditions; (*Lower*) Tax-KD conditions. (*B* and *C*) The time course of the absolute number (*B*) and fraction (*C*) of shNC (control) and shTax4 (Tax-KD) cells in a simulation resembling the experiment in Fig. 1*D*. In this simulated experiment, some MT-1 cells are shRNA+, and some are shRNA−. The simulated population dynamics of the shRNA+ cells in the mixed population are shown. The blue and green lines give the best fit solutions for the agent-based simulations based on Tax period sampling from experimental values (i.e., gray bars in Fig. S3*C*) and Tax interval sampling from simulated values (i.e., Fig. S3*G*). All data were fitted simultaneously. (*D*) The simulated dynamics of the frequency of Tax-expressing cells in the normal MT-1 cell population. A steady state is reached, in which about 3% of cells are Tax+. (*E* and *F*) The simulated dynamics of subpopulations of cells transduced with shNC (*E*, blue lines) or shTax4 (*F*, green lines). (*G*) The survival probabilities for subpopulations of shNC cells that have expressed Tax at least once and that have never expressed Tax are described by solid and dashed lines, respectively.

transient activation of retroviral LTRs and the maintenance of cell populations.

Tax expression is essential for de novo infection by HTLV-1, since viral transcription depends on Tax (30, 31). However, Tax expression strongly induces expression of viral proteins, including Tax, Env, and Gag, resulting in attacks by cytotoxic T lymphocytes (CTLs). Therefore, intermittent Tax expression is a clever strategy of HTLV-1 to evade the host immune response most of the time, but it maintains the ability to cause de novo infection under certain conditions. A recent study has reported that *tax* is induced by hypoxia (32); it is compatible with the previous observation that high *tax* expression was detected in the bone marrow, which is physiologically hypoxic (33). As another example, HTLV-1 can be transmitted through breastfeeding—a process in which HTLV-1–infected cells have to pass through the alimentary tract with acidic conditions and bile acids. Stress-induced Tax expression would be beneficial for de novo infection in these conditions. It is known that low pH and hypoxia in the physiological environment suppress adaptive immunity (34, 35), suggesting that infected cells may be able to "get away with" expressing Tax for a limited time in such immunological niches. To clarify the in vivo dynamics of Tax expression in immunocompetent hosts, additional studies using animal models will be required.

Tax expression is suppressed by genetic/epigenetic mechanisms in 50% of ATL cases (16, 36). The other one-half of ATL cases have the potential to express Tax, and indeed, it is known that nearly 50% of ATL cases express viral antigens after ex vivo culture (37). In this study, we show that survival of MT-1 cells, which express a level of *tax* similar to that of primary ATL cells (17), depends on Tax, suggesting that clinical ATL cases are divided into at least two classes: Tax-dependent and -independent ATL. A previous finding that the arsenic/IFN treatment induced apoptosis of several Tax-expressing cell lines, including MT-1, through degradation of Tax protein implies that those established cell lines still possess the characteristics of Tax-dependent ATL (38). It is known that the activity of Tax-specific CTLs is an important factor in inhibiting the onset of ATL (15). A recent study provided more evidence that Tax plays an important role in ATL: a clinical trial of a dendritic cell vaccine targeting Tax was efficacious (39). Tax expression was faint in fresh ATL cells of the enrolled patients, but it was inducible by ex vivo culture. These reports support our hypothesis that transiently expressed Tax plays critical roles in the development and maintenance of ATL, even if its expression is limited to a small fraction of leukemic cells. Recent comprehensive genomic studies of clinical ATL cases showed that genetic/epigenetic alterations accumulate in Tax-associated genes (40, 41), suggesting that the effects of these changes can substitute for Tax functions in leukemogenesis.

It is noteworthy that expression of *tax* was contrary to that of *HBZ*, even at the single-cell level ($r = -0.8$, $P < 0.0001$) (Fig. 2*D*). A similar observation in HTLV-1–infected T-cell clones was published while our study was under consideration for publication (42). That study showed the heterogeneity in the expression levels of *tax* and *HBZ* mRNA in fixed cells, whereas we here show the dynamics of Tax expression using live cell imaging. Tax and HBZ have opposing functions in many signaling pathways (9); however, the significance of their contrary activities has not been clarified. In this study, we found that Tax induces anti-apoptotic genes, such as *CFLAR*, *TNFRSF9*, *TRAF1*, and *TNFAIP3* (43–45). In contrast, pathways associated with cell proliferation, such as CD3, CD28, and melanogenesis-associated transcription factor (46, 47), are significantly activated in Tax-negative cells that express HBZ (Fig. 2*B*). This finding is compatible with the previous studies that showed that HBZ promotes T-cell growth by enhancing signals through CD3 and that KD of HBZ suppresses the proliferation of ATL cells, including MT-1 cells (12, 48, 49). The alternation of expression of Tax and HBZ seems to execute cooperative programs for survival and proliferation rather than cause them to interfere with each other. It has been reported that hyperactivation of the NF-κB pathway by Tax triggers senescence in HeLa cells, while HBZ could cancel this suppressive effect (27), suggesting that the collaboration of Tax and HBZ is important for the expansion of HTLV-1–infected cells. Transgenic mouse models have shown that both Tax and HBZ are oncogenic (50); however, their roles in HTLV-1–infected individuals are thought to be more complicated due to immune surveillance and the fact that human cells are more resistant to malignant transformation than rodent cells (51, 52). HBZ plays important roles in determining the immunophenotype of HTLV-1–infected cells, and HBZ itself has low immunogenicity (53, 54). It has been reported that the expression level of *HBZ* is higher in ATL cells than in nonleukemic infected cells, implying that infected clones with higher *HBZ* expression are selected during leukemogenesis (17). These findings suggest that constant expression of HBZ drives proliferation of cells with this specific immunophenotype, while transient Tax expression engages to inhibit cell death caused by various stresses. The different functions and expression patterns of Tax vs. HBZ are thought to be important in the malignant transformation of human T cells.

Recent studies show that many pathogens can persist in their reservoirs during both acute and chronic infections and reemerge

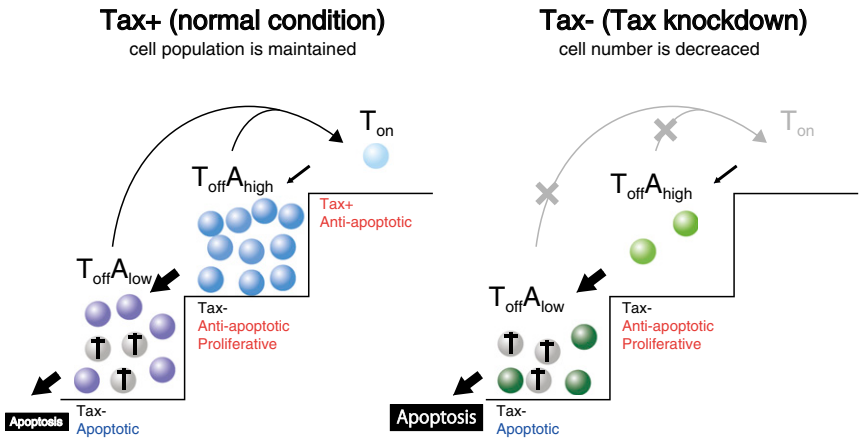

Fig. 6. Proposed model of the dynamics and significance of Tax expression. (*Left*) Under normal conditions; (*Right*) under Tax-KD conditions.

in the host under stressful conditions (55). In this study, we show that the HTLV-1 5′ LTR is activated by various cytotoxic stresses and several reagents that reactivate latent HIV (Fig. 3). These results suggest that HTLV-1–infected cells utilize mechanisms analogous to those of latent HIV-infected cells to act as reservoirs. One example is the antagonism of Tax and Tat to BRD4. BRD4 is a negative regulator of positive transcription elongation factor b (P-TEFb). It has been reported that both Tax and Tat compete with BRD4 for binding to P-TEFb (56, 57), and indeed, we found that a BRD4 inhibitor, JQ-1, efficiently reactivated the HTLV-1 5′ LTR (Fig. 3 *E* and *F* and Fig. S5*C*). These findings suggested that BRD4 can interrupt the positive feedback loop generated by the 5′ LTR and Tax/Tat and allow the establishment of latent infection by HTLV-1/HIV. Interestingly, many other viruses, including KSHV and human papilloma virus, also use BRD4 and/or P-TEFb to regulate viral lifecycles and pathogenesis (58–60). Identification of the cellular factors acted on by diverse viruses will contribute to exploring common mechanisms of viral latency and reactivation. In the case of HTLV-1, several repressors of viral replication, such as p30, Rex, and HBZ, are encoded in the provirus (9). These viral factors may be able to regulate the duration and/or timing of Tax expression in infected cells more elaborately. Additional investigation will be required to understand the precise roles of each protein in HTLV-1 latency.

Since the discovery of HTLV-1, a number of studies on its pathogenesis have been conducted; however, the prevention and treatment of HTLV-1–induced diseases are still unsatisfactory (61). In this study, we showed that sporadic and transient Tax expression in a small subset of cells has significant influence on gene expression of their progeny cells and consequently, maintains the whole population of ATL cells. This is a mechanism of the retrovirus for persistence and latency in vivo, and elucidation of this mechanism can contribute to a better understanding of viral pathogenesis and the development of strategies for treatment and prophylaxis of viral-associated diseases.

Materials and Methods

Cells. An IL-2–independent ATL cell line MT-1 (62), two IL-2–dependent ATL cell lines KK-1 and SO-4 (63), and an HTLV-1–negative T-cell line Jurkat were used in this study. MT-1 and Jurkat cells were maintained in RPMI supplemented with 10% (vol/vol) FBS. The MT1GFP cell line was maintained as MT-1 cells were, with the addition of 500 μg/mL G418 (Nacalai). KK-1 and SO-4 cell lines were maintained in RPMI supplemented with 10% FBS and IL-2 (100 U/mL; PeproTech).

Clinical Samples. Fresh ATL cells were obtained from 20 aggressive-type ATL cases and used for extraction of genomic DNA and total RNA. Use of the clinical samples in this research was approved by the Ethics Committee of Kyoto University (approval no. G204). Written consent was obtained from the patients. Using genomic DNAs from primary ATL cells and ATL cell lines, DNA methylation level of 5′ LTR was analyzed by the Combined Bisulfite Restriction Analysis method as previously described (36). Expression level of *tax* in fresh ATL cells was analyzed by a conventional qRT-PCR (16).

GFP Competition Assay. The GFP competition assay (64) was carried out to observe the long-term effect of Tax-KD on MT-1 or Jurkat cells transduced with pLKO-GFP lentivirus expressing shNC, shTax1, or shTax4. Cells were infected with concentrated lentivirus at a multiplicity of infection (MOI) of 0.5 to adjust the ratio of transduced cells to around 50%. The effect of shRNAs on target cells was evaluated by measuring the percentage of GFP+ cells using a FACSverse flow cytometer (BD Biosciences).

Single-Cell qPCR. The C1 Single-Cell Auto Prep Array for PreAmp (Fluidigm) was used for harvest of RNA, cDNA synthesis, and preamplification of cDNA (18 cycles of PCR for the target genes) from single cells according to the manufacturer's instructions. After loading cells onto an integrated fluidic circuit, we checked all 96 chambers by microscope to verify capture of a single cell. Thereafter, preamplified cDNA was harvested and subjected to qPCR. The Biomark HD system (Fluidigm) combined with EvaGreen chemistry (Bio-Rad) was used for the qPCR assay. To increase specificity, we used nested primers (one pair for the preamplification step and another pair for the subsequent qPCR of 30 cycles). The sequences of the primers used in this study are indicated in Table S3. Raw data were processed by Fluidigm Real-Time PCR analysis software, and the melting curve was used to determine the pass/failure call of qPCR. Data were analyzed with the R program using the Singular Analysis Toolset package (Fluidigm). Any chamber that contained more than one cell was excluded from analysis; outlier cells that had low global expression were also excluded. The level of detection value was set to 24 cycles according to the manufacturer's recommendation.

Time-Lapse Imaging. For live cell imaging, 8×10^4 MT1GFP cells were seeded in a 5-mm glass-bottom dish (Matsunami) precoated with poly-D-lysine (Sigma) and incubated at 37 °C in 5% CO_2. Images in the differential interference contrast (DIC) and GFP channels were captured with an LCV110 microscope (Olympus) every 20 min for 96 h. Semiautomated cell tracking was done by Fiji software with the Trackmate plugin (65). Cells, which had already expressed d2EGFP at the beginning of the observation, were excluded from analysis, because the starting point for expression was unknown. To analyze single-cell dynamics of d2EGFP expression, normalized fluorescence intensities are plotted against time. The starting time ($t = 0$) is the time at which the cell started expressing d2EGFP above background level.

RNA-Seq. MT1GFP or KK1GFP cells were sorted into d2EGFP+ and d2EGFP– populations with a FACSAria III (BD Biosciences), and RNA was then extracted using the RNeasy mini kit (Qiagen). Single-end RNA sequencing was performed (BGI). A quality check was done with FastQC, and then, Tuxedo pipeline was used for RNA quantification (66). Upstream regulator analysis was carried out by Ingenuity Pathway Analysis (Qiagen).

Cell Cycle Analysis. To measure the cell cycle dynamics of MT1GFP cells without cell synchronization, a method combining EdU incorporation and DAPI staining was carried out as previously described (25) using the Click-iT Plus EdU Alexa Fluor 647 kit (Thermo Fisher). Initially, 1×10^7 cells were cultured in complete RPMI medium containing 10 μM EdU for 2 h and washed thereafter. At that point (time = 2 h), one-half of the cells were fixed and stained for EdU and DAPI according to the manufacturer's protocol. The other one-half of the cells were recultured again for 4 h without adding EdU. At the end of the assay (time = 6 h), those cells were washed, fixed, and stained. Cell cycle status in the d2EGFP+ or d2EGFP– population was analyzed using a FACSVerse based on the levels of EdU and DAPI.

Statistical Analysis. Statistical analysis was done using Microsoft Excel, GraphPad Prism, R, or Python. Data obtained by flow cytometry were analyzed with FlowJo. Two-sided *t* test was used to compare between two different groups.

Computational Simulations. A simple deterministic two-state model of Tax-positive feedback was developed (the chemical reaction scheme is shown in Fig. S3*A*) (19) and simulated by the Gillespie algorithm (67) to investigate the stochastic dynamics of Tax expression, especially to estimate the length of Tax expression (t_{period}) and the interval between Tax expression episodes ($t_{interval}$). In addition, an ABM of cell population dynamics (birth–death Poisson process) with stage transitions as described in Fig. 5*A* was constructed based on the individual-based Gillespie algorithm (67) to confirm the experiment-based hypothesis that the transient expression of Tax is a critical event for the persistence of the MT-1 cell population. Additional details are in *SI Materials and Methods*.

ACKNOWLEDGMENTS. We thank Dr. Mitsuaki Yoshida (The Cancer Institute, Japanese Foundation for Cancer Research) for helpful discussion, Dr. Chou-Zen Giam (Uniformed Services University of the Health Sciences) for providing PB-18X21-RFP and PB-Tase, Drs. Hiroo Hasegawa and Yasuaki Yamada (Nagasaki University) for KK-1 and SO-4, and Dr. Linda Kingsbury for proofreading. This study was supported by Japan Society for the Promotion of Science (JSPS) KAKENHI Grants JP16H05336 (to M. Matsuoka), 26460554 and JP17K07166 (to J.-i.Y.), and JP15H05707 and JP16K05265 (to S.N.); Project for Cancer Research and Therapeutic Evolution Grant 17cm0106306h0002 (to J.-i.Y. and M. Matsuoka); Research Program on Emerging and Re-Emerging Infectious Diseases Grant 17fk0108227h0002 (to J.-i.Y. and M. Matsuoka) and Japanese Initiative for Progress of Research on Infectious Disease for Global Epidemics (J-PRIDE) Grants 17fm0208006h0001 (to S.I.), 17fm0208019h0101 (to S.I.), and 17fm0208014h0001 (to S.I.) from the Japan Agency for Medical Research and Development; a grant from the Princess Takamatsu Cancer Research Fund (to J.-i.Y.); a grant from The Yasuda Medical Foundation (to J.-i.Y.); the Japan Science and Technology Agency (JST) Precursory Research for Embryonic Science and Technology

(PRESTO) [S.I., and Grant JPMJPR16E9 (to S.N.)] and Core Research for Evolutional Science and Technology (CREST) Programs (S.I.); and Grants-in-Aid for Scientific Research on Innovative Areas 16H06429 (S.I.), 16K21723 (S.I.), and 17H05819 (to S.I.) from Ministry of Education, Culture, Sports, Science, and Technology (MEXT). This study was also supported in part by the JSPS Core-to-Core Program A, Advanced Research Networks.

1. Virgin HW, Wherry EJ, Ahmed R (2009) Redefining chronic viral infection. *Cell* 138: 30–50.
2. Traylen CM, et al. (2011) Virus reactivation: A panoramic view in human infections. *Future Virol* 6:451–463.
3. Mesri EA, Feitelson MA, Munger K (2014) Human viral oncogenesis: A cancer hallmarks analysis. *Cell Host Microbe* 15:266–282.
4. Tagaya Y, Gallo RC (2017) The exceptional oncogenicity of HTLV-1. *Front Microbiol* 8: 1425.
5. Matsuoka M, Jeang KT (2007) Human T-cell leukaemia virus type 1 (HTLV-1) infectivity and cellular transformation. *Nat Rev Cancer* 7:270–280.
6. Demontis MA, Sadiq MT, Golz S, Taylor GP (2015) HTLV-1 viral RNA is detected rarely in plasma of HTLV-1 infected subjects. *J Med Virol* 87:2130–2134.
7. Melamed A, et al. (2013) Genome-wide determinants of proviral targeting, clonal abundance and expression in natural HTLV-1 infection. *PLoS Pathog* 9:e1003271.
8. Philip S, Zahoor MA, Zhi H, Ho YK, Giam CZ (2014) Regulation of human T-lymphotropic virus type I latency and reactivation by HBZ and Rex. *PLoS Pathog* 10: e1004040.
9. Matsuoka M, Yasunaga J (2013) Human T-cell leukemia virus type 1: Replication, proliferation and propagation by tax and HTLV-1 bZIP factor. *Curr Opin Virol* 3: 684–691.
10. Boxus M, et al. (2008) The HTLV-1 tax interactome. *Retrovirology* 5:76.
11. Hanon E, et al. (2000) Abundant tax protein expression in CD4+ T cells infected with human T-cell lymphotropic virus type I (HTLV-I) is prevented by cytotoxic T lymphocytes. *Blood* 95:1386–1392.
12. Satou Y, Yasunaga J, Yoshida M, Matsuoka M (2006) HTLV-I basic leucine zipper factor gene mRNA supports proliferation of adult T cell leukemia cells. *Proc Natl Acad Sci USA* 103:720–725.
13. Jacobson S, Shida H, McFarlin DE, Fauci AS, Koenig S (1990) Circulating CD8+ cytotoxic T lymphocytes specific for HTLV-I pX in patients with HTLV-I associated neurological disease. *Nature* 348:245–248.
14. Kannagi M, et al. (1991) Predominant recognition of human T cell leukemia virus type I (HTLV-I) pX gene products by human CD8+ cytotoxic T cells directed against HTLV-I-infected cells. *Int Immunol* 3:761–767.
15. Kannagi M, Hasegawa A, Takamori A, Kinpara S, Utsunomiya A (2012) The roles of acquired and innate immunity in human T-cell leukemia virus type 1-mediated diseases. *Front Microbiol* 3:323.
16. Takeda S, et al. (2004) Genetic and epigenetic inactivation of tax gene in adult T-cell leukemia cells. *Int J Cancer* 109:559–567.
17. Usui T, et al. (2008) Characteristic expression of HTLV-1 basic zipper factor (HBZ) transcripts in HTLV-1 provirus-positive cells. *Retrovirology* 5:34.
18. Zhang L, Liu M, Merling R, Giam CZ (2006) Versatile reporter systems show that transactivation by human T-cell leukemia virus type 1 Tax occurs independently of chromatin remodeling factor BRG1. *J Virol* 80:7459–7468.
19. Razooky BS, Pai A, Aull K, Rouzine IM, Weinberger LS (2015) A hardwired HIV latency program. *Cell* 160:990–1001.
20. Marullo R, et al. (2013) Cisplatin induces a mitochondrial-ROS response that contributes to cytotoxicity depending on mitochondrial redox status and bioenergetic functions. *PLoS One* 8:e81162.
21. Valerie K, et al. (1988) Activation of human immunodeficiency virus type 1 by DNA damage in human cells. *Nature* 333:78–81.
22. Legrand-Poels S, Vaira D, Pincemail J, van de Vorst A, Piette J (1990) Activation of human immunodeficiency virus type 1 by oxidative stress. *AIDS Res Hum Retroviruses* 6:1389–1397.
23. Zhu J, et al. (2012) Reactivation of latent HIV-1 by inhibition of BRD4. *Cell Rep* 2: 807–816.
24. Weinberger LS, Burnett JC, Toettcher JE, Arkin AP, Schaffer DV (2005) Stochastic gene expression in a lentiviral positive-feedback loop: HIV-1 Tat fluctuations drive phenotypic diversity. *Cell* 122:169–182.
25. Fleisig H, Wong J (2012) Measuring cell cycle progression kinetics with metabolic labeling and flow cytometry. *J Vis Exp* e4045.
26. Kinjo T, Ham-Terhune J, Peloponese JM, Jr, Jeang KT (2010) Induction of reactive oxygen species by human T-cell leukemia virus type 1 tax correlates with DNA damage and expression of cellular senescence marker. *J Virol* 84:5431–5437.
27. Zhi H, et al. (2011) NF-κB hyper-activation by HTLV-1 tax induces cellular senescence, but can be alleviated by the viral anti-sense protein HBZ. *PLoS Pathog* 7:e1002025.
28. Zalzman M, et al. (2010) Zscan4 regulates telomere elongation and genomic stability in ES cells. *Nature* 464:858–863.
29. Eckersley-Maslin MA, et al. (2016) MERVL/Zscan4 network activation results in transient genome-wide DNA demethylation of mESCs. *Cell Rep* 17:179–192.
30. Cann AJ, Rosenblatt JD, Wachsman W, Shah NP, Chen IS (1985) Identification of the gene responsible for human T-cell leukaemia virus transcriptional regulation. *Nature* 318:571–574.
31. Felber BK, Paskalis H, Kleinman-Ewing C, Wong-Staal F, Pavlakis GN (1985) The pX protein of HTLV-I is a transcriptional activator of its long terminal repeats. *Science* 229:675–679.
32. Kulkarni A, et al. (2017) Glucose metabolism and oxygen availability govern reactivation of the latent human retrovirus HTLV-1. *Cell Chem Biol* 24:1377–1387.e3.
33. Levin MC, et al. (1997) Extensive latent retroviral infection in bone marrow of patients with HTLV-I-associated neurologic disease. *Blood* 89:346–348.
34. Kareva I, Hahnfeldt P (2013) The emerging "hallmarks" of metabolic reprogramming and immune evasion: Distinct or linked? *Cancer Res* 73:2737–2742.
35. Taylor CT, Colgan SP (2017) Regulation of immunity and inflammation by hypoxia in immunological niches. *Nat Rev Immunol* 17:774–785.
36. Taniguchi Y, et al. (2005) Silencing of human T-cell leukemia virus type I gene transcription by epigenetic mechanisms. *Retrovirology* 2:64.
37. Kurihara K, et al. (2005) Potential immunogenicity of adult T cell leukemia cells in vivo. *Int J Cancer* 114:257–267.
38. Dassouki Z, et al. (2015) ATL response to arsenic/interferon therapy is triggered by SUMO/PML/RNF4-dependent Tax degradation. *Blood* 125:474–482.
39. Suehiro Y, et al. (2015) Clinical outcomes of a novel therapeutic vaccine with Tax peptide-pulsed dendritic cells for adult T cell leukaemia/lymphoma in a pilot study. *Br J Haematol* 169:356–367.
40. Kataoka K, et al. (2015) Integrated molecular analysis of adult T cell leukemia/lymphoma. *Nat Genet* 47:1304–1315.
41. Fujikawa D, et al. (2016) Polycomb-dependent epigenetic landscape in adult T-cell leukemia. *Blood* 127:1790–1802.
42. Billman MR, Rueda D, Bangham CRM (2017) Single-cell heterogeneity and cell-cycle-related viral gene bursts in the human leukaemia virus HTLV-1. *Wellcome Open Res* 2: 87.
43. Okamoto K, Fujisawa J, Reth M, Yonehara S (2006) Human T-cell leukemia virus type-I oncoprotein tax inhibits Fas-mediated apoptosis by inducing cellular FLIP through activation of NF-kappaB. *Genes Cells* 11:177–191.
44. Saitoh Y, et al. (2016) A20 targets caspase-8 and FADD to protect HTLV-I-infected cells. *Leukemia* 30:716–727.
45. Sabbagh L, et al. (2013) Leukocyte-specific protein 1 links TNF receptor-associated factor 1 to survival signaling downstream of 4-1BB in T cells. *J Leukoc Biol* 93:713–721.
46. Acuto O, Michel F (2003) CD28-mediated co-stimulation: A quantitative support for TCR signalling. *Nat Rev Immunol* 3:939–951.
47. Flaherty KT, Hodi FS, Fisher DE (2012) From genes to drugs: Targeted strategies for melanoma. *Nat Rev Cancer* 12:349–361.
48. Arnold J, Zimmerman B, Li M, Lairmore MD, Green PL (2008) Human T-cell leukemia virus type-1 antisense-encoded gene, Hbz, promotes T-lymphocyte proliferation. *Blood* 112:3788–3797.
49. Kinosada H, et al. (2017) HTLV-1 bZIP factor enhances T-cell proliferation by impeding the suppressive signaling of co-inhibitory receptors. *PLoS Pathog* 13:e1006120.
50. Yasunaga J, Matsuoka M (2011) Molecular mechanisms of HTLV-1 infection and pathogenesis. *Int J Hematol* 94:435–442.
51. Hahn WC, et al. (1999) Creation of human tumour cells with defined genetic elements. *Nature* 400:464–468.
52. Grassmann R, Aboud M, Jeang KT (2005) Molecular mechanisms of cellular transformation by HTLV-1 Tax. *Oncogene* 24:5976–5985.
53. Bangham CRM, Matsuoka M (2017) Human T-cell leukaemia virus type 1: Parasitism and pathogenesis. *Philos Trans R Soc Lond B Biol Sci* 372:20160272.
54. Ma G, Yasunaga J, Matsuoka M (2016) Multifaceted functions and roles of HBZ in HTLV-1 pathogenesis. *Retrovirology* 13:16.
55. Anonymous (2017) Lessons from reservoirs. *Nat Med* 23:899.
56. Bisgrove DA, Mahmoudi T, Henklein P, Verdin E (2007) Conserved P-TEFb-interacting domain of BRD4 inhibits HIV transcription. *Proc Natl Acad Sci USA* 104:13690–13695.
57. Cho WK, et al. (2007) Modulation of the Brd4/P-TEFb interaction by the human T-lymphotropic virus type 1 tax protein. *J Virol* 81:11179–11186.
58. Chen HS, et al. (2017) BET-inhibitors disrupt Rad21-dependent conformational control of KSHV latency. *PLoS Pathog* 13:e1006100.
59. Jang MK, Shen K, McBride AA (2014) Papillomavirus genomes associate with BRD4 to replicate at fragile sites in the host genome. *PLoS Pathog* 10:e1004117.
60. Zaborowska J, Isa NF, Murphy S (2016) P-TEFb goes viral. *Inside Cell* 1:106–116.
61. Willems L, et al. (2017) Reducing the global burden of HTLV-1 infection: An agenda for research and action. *Antiviral Res* 137:41–48.
62. Miyoshi I, et al. (1980) A novel T-cell line derived from adult T-cell leukemia. *Gan* 71: 155–156.
63. Yamada Y, et al. (1998) Interleukin-15 (IL-15) can replace the IL-2 signal in IL-2-dependent adult T-cell leukemia (ATL) cell lines: Expression of IL-15 receptor alpha on ATL cells. *Blood* 91:4265–4272.
64. Eekels JJ, et al. (2012) A competitive cell growth assay for the detection of subtle effects of gene transduction on cell proliferation. *Gene Ther* 19:1058–1064.
65. Jaqaman K, et al. (2008) Robust single-particle tracking in live-cell time-lapse sequences. *Nat Methods* 5:695–702.
66. Trapnell C, et al. (2012) Differential gene and transcript expression analysis of RNA-seq experiments with TopHat and Cufflinks. *Nat Protoc* 7:562–578.
67. Gillespie DT (1976) A general method for numerically simulating the stochastic time evolution of coupled chemical reactions. *J Comput Phys* 22:403–434.

Supporting Information

Mahgoub et al. 10.1073/pnas.1715724115

SI Materials and Methods

Plasmids. The *Piggy*Bac Transposon system (System Biosciences) was used in this study. A Tax-responsive element (TRE)-driven reporter plasmid, PB-18 × 21-RFP, and a transposase expression vector, PB-Tase, were provided by Chou-Zen Giam, Uniformed Services University of Health Sciences, Bethesda (1). To obtain d2EGFP under the control of the TREs, we generated PB-18 × 21-d2EGFP from PB-18 × 21-RFP and pd2EGFP (Clontech) by replacing the coding sequence of RFP with the fragment containing d2EGFP and the neomycin resistance gene. The 2A peptide-based bicistronic construct expressing Tax (or Tat) and d2EGFP through the HTLV-1 5′ LTR (or HIV 5′ LTR) replaced the CMV promoter of PB-CMV-MCS-EF1-Puro (System Biosciences) to produce PB-HTLV-1 LTR-d2EGFP Tax and PB-HIV LTR-d2EGFP Tat, respectively. For KD experiments, lentivirus vectors expressing shRNAs were used. For shRNAs, a fragment targeting a Tax coding sequence (shTax1: gccttcctcaccaatgttc or shTax4: ggcagatgacaatgaccatga) or a nontarget shRNA (shNC: caacaagatgaagagcaccaa) was inserted into pLKO.1-EGFP (Sigma-Aldrich).

Transfection and Lentivirus Transduction. We stably transfected MT-1 cells with the reporter transposon PB-18 × 21-d2EGFP using the Neon Transfection System (Thermo Fisher Scientific), thus generating MT1GFP cells; 5×10^5 MT-1 cells were electroporated with 1 μg of PB-18 × 21-d2EGFP and 0.3 μg of PB-Tase helper plasmid. Forty-eight hours later, G418 (1,000 μg/mL) was added for selection. Stable clones were isolated by limiting dilution and expanded in 96-well plates. For lentivirus production, 3–5 × 10^6 of HEK293T cells were seeded in a 10-cm dish, and 24 h later, they were transfected with 15 μg of HIV Gag/Pol-expression plasmid (pCMVΔ8/9), 7.5 μg of Env expression plasmid (pVSV-G), and 15 μg of shRNA-expressing plasmid (pLKO-GFP-shRNA). Polyethylenimine (PEI MAX 40000 from Polysciences) was used for packaging of the lentivirus vectors. Forty-eight hours after transfection, the supernatant was collected and concentrated using ultracentrifugation; 3×10^5 MT-1 or Jurkat cells were seeded in 12-well plates and infected with the concentrated virus.

Flow Cytometry. To measure GFP expression, cells were washed once with FACS buffer (PBS + 2% FBS) and analyzed with a FACSVerse directly or after staining with LIVE/DEAD Near-IR (Molecular Probes) for viability. For apoptosis, cells were stained with Alexa Fluor 647 Annexin V and 7-AAD (Biolegend). For intracellular staining of Tax, cells were fixed and permeabilized with the Foxp3 Intracellular Staining Buffer Set (eBioscience) and then stained with anti-Tax mouse monoclonal antibody (clone MI73) and anti-Mouse IgG Alexa Fluor 647 (Life Technologies). Cells were also stained with DAPI to exclude sub-G1 dead cells.

Stochastic Simulation of Intracellular Tax Expression Model. A previous study on HIV elegantly established a mathematical model of 5′ LTR activation by Tat in latently infected cells (2). We adapted this model to simulate the regulation of the HTLV-1 5′ LTR by Tax (Fig. S3*A* shows a schematic representation). We tested several parameters used in the HIV study and adjusted them to fit our experimental data of transient Tax expression (Fig. S3 *B–D* and Table S1) (see below). A simple deterministic two-state model of Tax-positive feedback was developed (the chemical reaction scheme is shown in Fig. S3*A*) (2). A stochastic simulation model corresponding to the deterministic two-state model was constructed and implemented by the Gillespie algorithm (3) to investigate the stochastic dynamics of Tax expression, especially for the length of Tax expression (t_{period}) and the interval between Tax expression periods (t_{interval}):

$$\frac{d}{dt}[5'LTR_{OFF}] = -k_{ON}[5'LTR_{OFF}] + k_{OFF}[5'LTR_{ON}] - k_{\text{bind}}[5'LTR_{ON}][Tax] + k_{\text{unbind}}[5'LTR_{ON-Tax}],$$

$$\frac{d}{dt}[5'LTR_{ON}] = k_{ON}[5'LTR_{OFF}] - k_{OFF}[5'LTR_{ON}],$$

$$\frac{d}{dt}[mRNA] = k_m[5'LTR_{ON}] + k_a[5'LTR_{ON-Tax}] - \delta_m[mRNA],$$

$$\frac{d}{dt}[Tax] = k_p[mRNA] - k_{\text{bind}}[5'LTR_{OFF}][Tax] + k_{\text{unbind}}[5'LTR_{ON-Tax}] - \delta_p[Tax],$$

$$\frac{d}{dt}[5'LTR_{ON-Tax}] = k_{\text{bind}}[5'LTR_{OFF}][Tax] - k_{\text{unbind}}[5'LTR_{ON-Tax}].$$

The description of the chemical reaction scheme and parameter values used in our simulations is summarized in Table S1. The Gillespie direct method was coded in C++ (the source code is freely available at https://github.com/petadimension/Tax_dynamics/) to achieve fast and efficient computations. Each stochastic simulation was performed until a computational time of 100,000. An arbitrarily chosen timescale factor 0.00065 was multiplied with the computational time to imitate the experimental time period for the live cell imaging (65 h as a maximum period). Initial conditions for all chemical reaction agents were set to zero, except for $5'LTR_{ON}$ (the second variable in the deterministic model), which was set to one. A sample path of Tax protein population (the fourth variable in the deterministic model) is presented in Fig. S3*B*.

Fitting Mathematical Model to Data. Simulated Tax periods generated from the stochastic simulation model were fitted to the distribution of experimentally observed Tax periods (gray bars in Fig. S3*C*). Using the "entropy" package of statistical software R (4), we calculated the discretized Kullback–Leibler divergence for simulated and experimental data of Tax periods with equal-sized 10 bins (7 h each) to evaluate the closeness of fit between the simulation and experimental data. In fitting, all of the parameters except for k_{bind} and k_{unbind} were kept fixed to the reference value (Table S1). A brute force computation of closeness was performed on a uniform 16 × 16 grid of $(k_{\text{bind}}, k_{\text{unbind}})$, where the ranges of k_{bind} and k_{unbind} are set to [0.0005, 0.04] and [0.005, 0.04], respectively. The ranking of closeness (ranking 1–256) is presented in Fig. S3*D*.

Agent-Based Simulation of Cell Population Dynamics. The ABM simulating the population dynamics of MT-1 cells transfected with shRNA as a Poisson (birth–death) process with a stage transition as described in Fig. S5*A* was constructed based on the individual-based Gillespie algorithm: an extension of the conventional Gillespie algorithm (3), which allows one to include nonexponentially distributed waiting times of event occurrences as a nonhomogeneous Poisson process (5). Possible events include cell division, death, and stage transitions among three cell

types. The ABM that we constructed describes cell division and death events as a Poisson process with the growth rate parameter $g = 0.68$ for both Tax-negative cells expressing high levels of antiapoptotic genes ($T_{off}A_{high}$ cells) and Tax-negative antiapoptotic gene expression low ($T_{off}A_{low}$) cells as well as the growth rate parameter $g_{on} = 0.54$ for Tax-expressing (T_{on}) cells. The lower value for the g_{on} parameter reflects our experimental observation that the transition to G2/M occurs only 80% as quickly in T_{on} cells (Fig. 4). We used the death rate parameter $\delta = 0.25$ for $T_{off}A_{low}$ cells. The stage transition of Tax-negative cells from antiapoptotic gene expression high to low is also described by a Poisson process with rate parameters $p = 0.02$ and $p^* = 0.40$ for shNC and shTax4 cells, respectively. Note that the parameters governing the rates of other stage transitions (i.e., the transition from Tax_{on} to Tax_{off} and vice versa) need to be determined based on sampling from experimental (or previously simulated) Tax period/Tax interval data, which would be appropriately fitted with nonexponential distributions. In fact, our ABM allows us to include sampling of arbitrary waiting times (Tax periods and intervals) from experimental (or previously simulated) data. We summarize the parameter values in Table S2.

To simulate and reproduce the dynamics of shRNA-transduced cells growing in a mixture with untransduced cells, we need also to consider the growth rate of the untransduced cells. Untransduced MT-1 cells would show the same population dynamics as shNC-transduced cells in our ABM. Numerical simulation results from our ABM exhibit transient behaviors until day 3 due to demographic stochasticity when the number of cells is small (i.e., around 10 cells). However, after this transient phase, a steady-state phase is reached, in which our numerical results are quite stable. Hence, we started our ABM after day 3 to avoid possible artifacts due to demographic stochasticity in a transient phase. We fixed the initial numbers of MT-1 cells with and without shRNA at day 3 at 104 and 63, respectively. (The corresponding expected numbers of cells at day 0 are 12 and 11, respectively.) The initial conditions of ABM simulation were set as follows. For both shNC and shTax4 cells, less than 10% of the total cell population are T_{on}. However, we assumed that large and small fractions of the total cell population consist of $T_{off}A_{high}$ for shNC and shTax4 cells (78 and 2%, respectively). This is because we needed to consider the effect of Tax-KD on the expression of antiapoptotic genes. We also confirmed that the choice of these values is not qualitatively essential in a steady-state phase (results not shown). ABM simulations for mixtures of MT-1 cells with and without shRNA were performed until day 21. Simulation results with Tax period sampling from experimental and simulated values for shNC and shTax4 cells are shown in Fig. 5 and Fig. S6, respectively.

Since the total number of MT-1 cells without shRNA reaches 10^4 around day 10, the propensities of cell division, death, and transition rarely change. In other words, the propensities required to determine the relative occurrence of an event to be selected in the Gillespie algorithm remain almost constant for a period of computational time. This allows us to skip updating the propensities, which efficiently reduces computational time. Hence, we adopted an approximation algorithm to update propensities only once every 10,000 events if the total cell number exceeds 10^4 (after day 10) and confirmed that this approximation does not affect population dynamics. The ABM is coded and implemented by statistical software R. (The source code is available at https://github.com/petadimension/Tax_dynamics/tree/master/ABM.)

Survival Probability for Subpopulations. We performed a tracking simulation for the shNC population to investigate the difference in survival time among subpopulations. Note that, in this simulation, subpopulations are defined as Tax experienced (cells in which Tax has already been expressed at least once) or Tax naïve (cells in which Tax has never been expressed). Let a denote the age of a daughter cell, which corresponds to the time since a mother cell divided. Since we were calculating survival probabilities, we only needed to track the survival of one cohort: a subgroup of cells with the same age a. In the tracking simulation, we recorded the times of cell death and the statuses of all cells, and we produced probability density distributions $f_i(a)$ for the survival time of the Tax experienced $(i = e)$ and naïve $(i = n)$ subpopulations. Survival probabilities are then derived as $F_i(a) = 1 - \int_0^a f_i(s)ds$ (6). In this tracking simulation, we used the same parameter values that we used in the ABM simulations (see above) (Table S2), except for the growth rate ($g = 0$ for the tracking simulation, because tracking requires only one cohort) and the initial number of a target cohort, which is set to 10,000. Survival probability curves of the two subpopulations are shown in Fig. 5*G*: about 90% of Tax nonexperienced cells die within 2 wk, but Tax experienced cells survive much longer, suggesting that Tax expression can make a significant contribution to cell survival.

1. Zahoor MA, Philip S, Zhi H, Giam CZ (2014) NF-κB inhibition facilitates the establishment of cell lines that chronically produce human T-lymphotropic virus type 1 viral particles. *J Virol* 88:3496–3504.
2. Razooky BS, Pai A, Aull K, Rouzine IM, Weinberger LS (2015) A hardwired HIV latency program. *Cell* 160:990–1001.
3. Gillespie DT (1976) A general method for numerically simulating the stochastic time evolution of coupled chemical reactions. *J Comput Phys* 22:403–434.
4. R Core Team (2017) R: A Language and Environment for Statistical Computing. Available at www.R-project.org/. Version 3.3.3.
5. Nakaoka S, Aihara K (2013) Stochastic simulation of structured skin cell population dynamics. *J Math Biol* 66:807–835.
6. Aalen O, Borgan O, Gjessing H (2008) *Survival and Event History Analysis: A Process Point of View* (Springer Science & Business Media, New York).

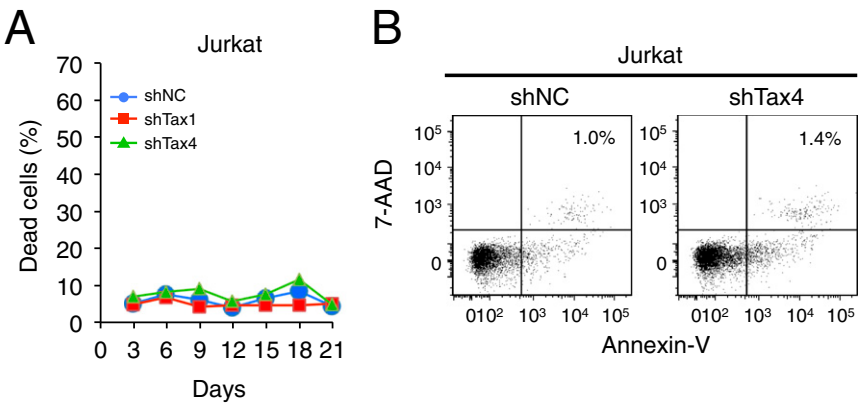

Fig. S1. Effects of shRNAs against Tax on HTLV-1–uninfected cells. (*A*) Tax-KD does not cause apoptosis in uninfected cells. Jurkat cells were transduced with anti-Tax shRNA or control nontarget shRNA. The percentage of dead cells in the transduced (GFP+) population was measured by flow cytometry using LIVE/DEAD reagent. (*B*) AnnexinV/7-AAD double staining in shRNA-transduced Jurkat cells at day 15 posttransduction.

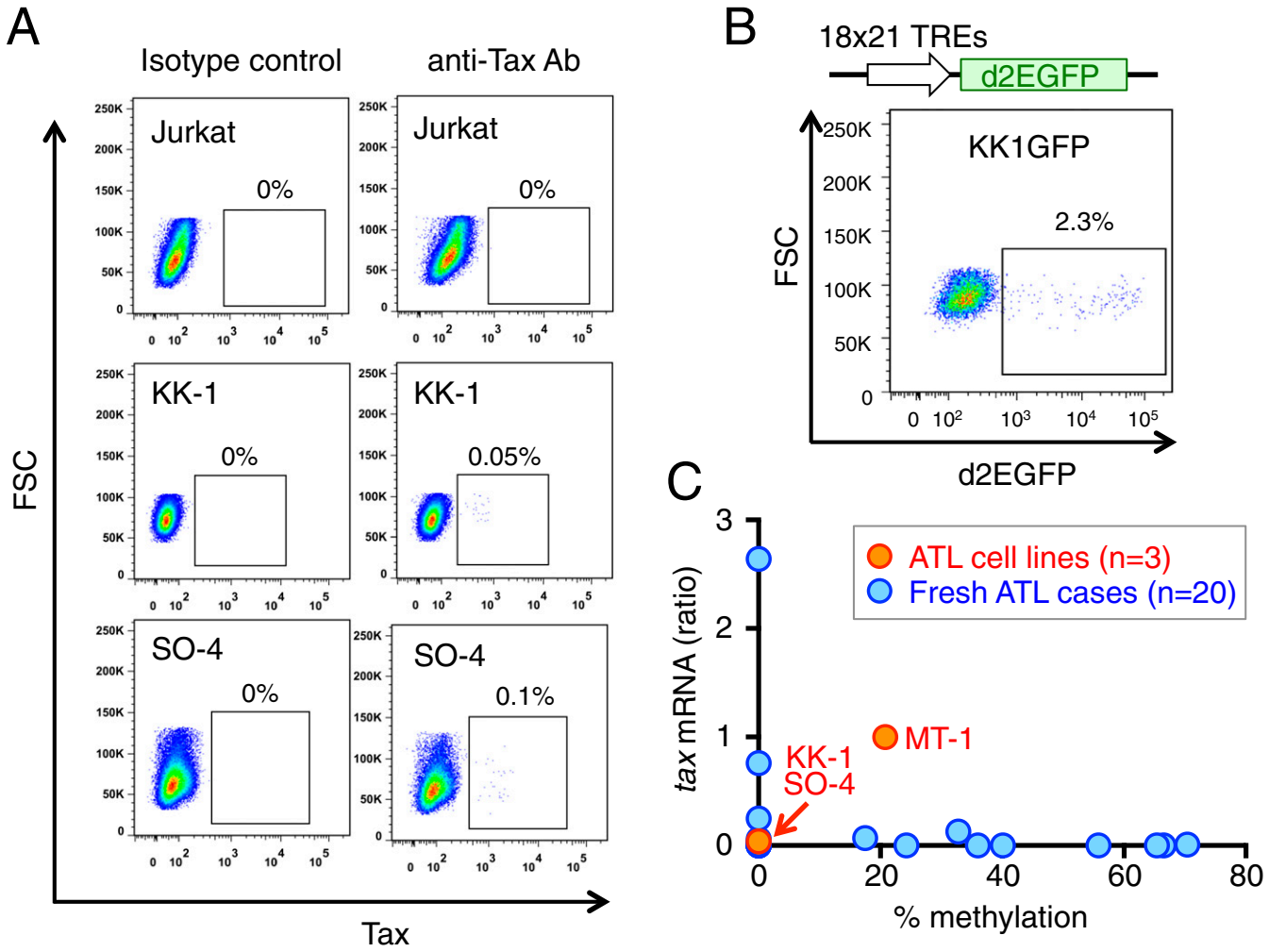

Fig. S2. Tax expression in several ATL cell lines. (*A*) Intracellular Tax staining in ATL cells lines KK-1and SO-4 and an HTLV-1–negative T-cell line Jurkat. FSC, forward scatter. (*B*) Generation of a Tax reporter subline of KK-1 (KK1GFP). (*Upper*) Scheme of the reporter cassette expressing d2EGFP under the control of tandem repeats of TRE. (*Lower*) Expression of d2EGFP in a representative subclone of KK1GFP. (*C*) Correlation between levels of *tax* mRNA and DNA methylation of 5′ LTR in fresh ATL cells and ATL cell lines. Fresh ATL cells from aggressive-type ATL (n = 20) and three ATL cell lines (MT-1, KK-1, and SO-4) were subjected to the analysis.

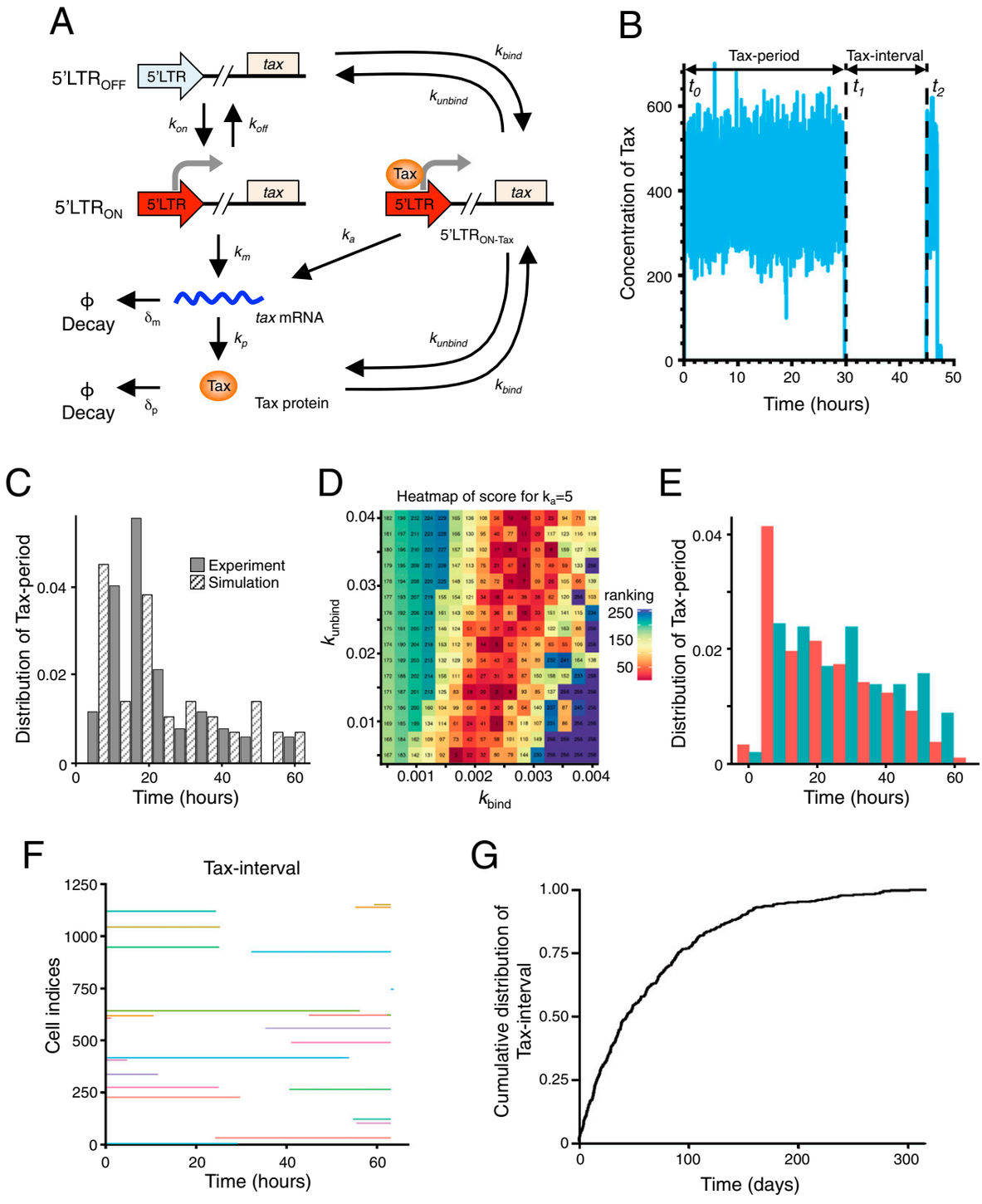

Fig. S3. Computational simulation of intracellular Tax expression dynamics. (*A*) Scheme for the mathematical modeling of the Tax expression process. (*B*) A sample path of the stochastic simulation of the Tax expression process. The *Tax period* is defined as the time period of sustained Tax expression between the start point (the first time to reach the burst threshold of 200 copies from no expression) and the end point (the time to return to no expression; i.e., $t_{\text{period}} = t_1 - t_0$). The *Tax interval* is defined as the time from the end of one Tax period to the beginning of the next (the time during which the Tax concentration never reaches the burst threshold; i.e., $t_{\text{interval}} = t_2 - t_1$). (*C*) The experimental and simulation-predicted distributions of Tax period durations are shown. (*D*) The ranking of feasible parameter sets determined by computing the closeness of simulated and experimentally determined Tax periods. For each choice of the two parameters k_{bind} and k_{unbind}, a distribution of Tax periods was generated by a single long-run stochastic simulation (up to 1.0×10^8 h). The closeness between simulated and experimental Tax periods was then numerically computed by the discretized Kullback–Leibler divergence (R package entropy). The ranking is determined by the closeness: the box with the minimum Kullback–Leibler divergence value is ranked one. If no Tax periods are found, the maximum Kullback–Leibler divergence value is assigned (boxes with ranking 256). (*E*) Comparison of histograms for the distribution of Tax periods between the collection of short-run (up to 65 h) and long-run (65,000 h) stochastic simulations. A total of 362 Tax periods from 10,000 short-run simulations are used (red bars), while 407 Tax periods were obtained from a single long-run simulation (blue bars). (*F*) Plots of Tax periods generated from short-run stochastic simulations. Twenty-four samples that exhibit a Tax interval are mapped on the time axis. (*G*) The simulation-predicted cumulative distribution of Tax intervals is shown; 50% of Tax intervals are longer than about 40 d.

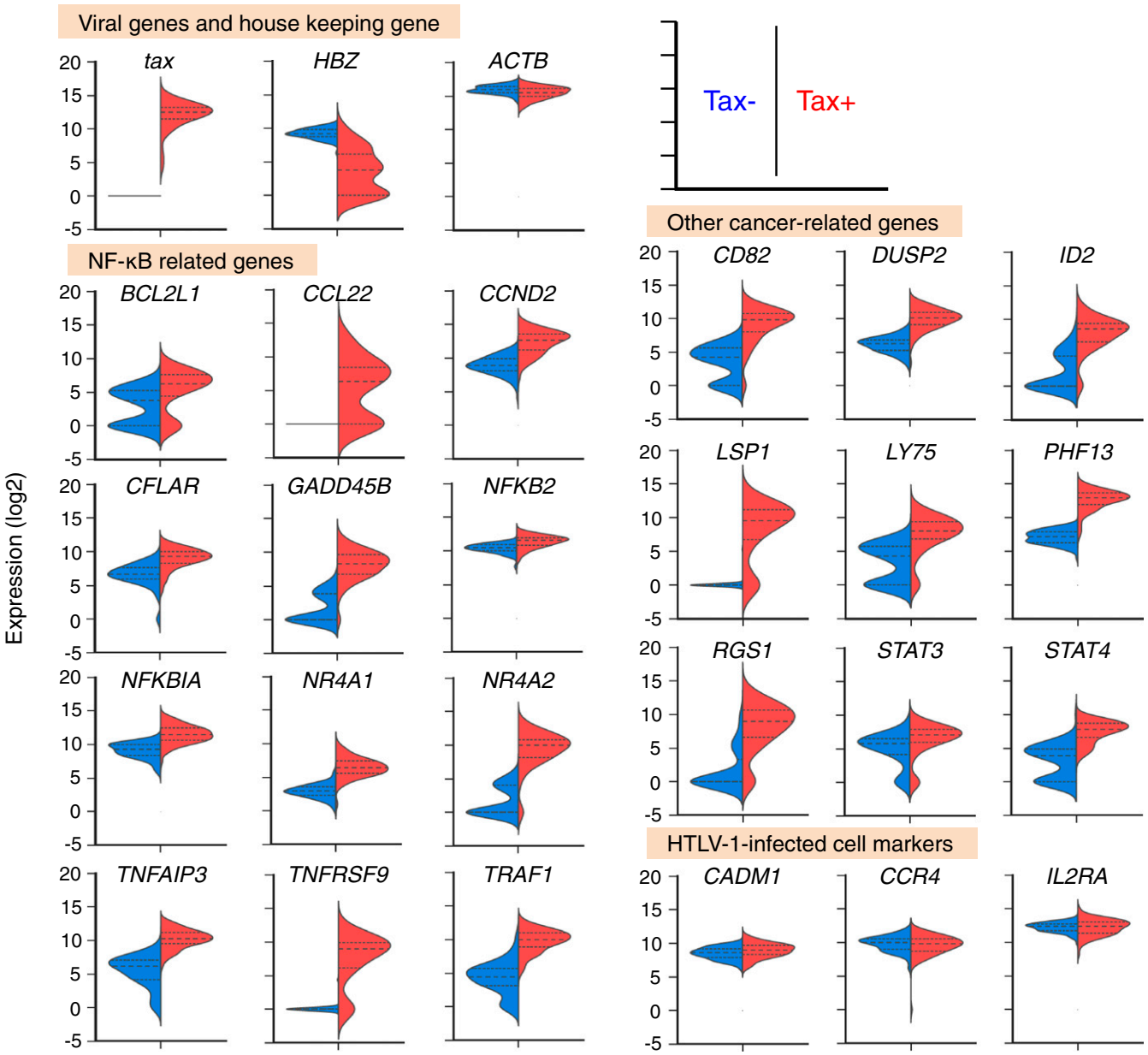

Fig. S4. Violin plots of genes expressed differentially in Tax+ and Tax– MT1GFP cells. Results of single-cell qPCR for the selected genes are shown as violin plots. Inner lines represent the population's distribution percentiles: (top line) 75th; (middle line) 50th; and (bottom line) 25th.

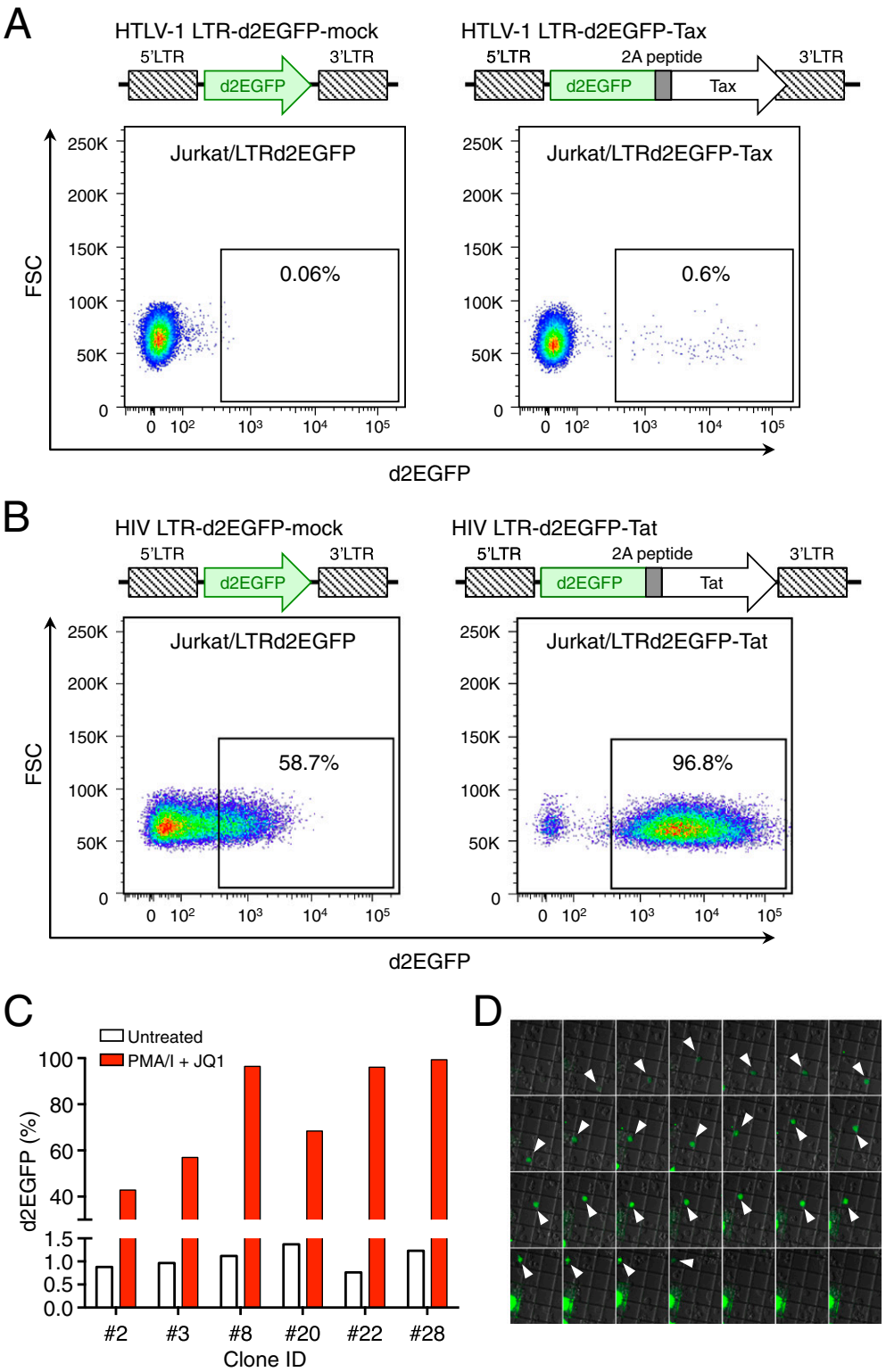

Fig. S5. Latent phenotype established by HTLV-1-LTR Tax minimal circuit. (*A* and *B*) d2EGFP expression under the control of the LTR promoter from HTLV-1 or HIV-1 in the presence or absence of transactivator (Tax or Tat, respectively) in stably transfected Jurkat cells. (*A*) d2EGFP expression from the HTLV-1 LTR: basal transcription (*Left*) and transcription in the presence of Tax-positive feedback (*Right*). (*B*) d2EGFP expression from the HIV-1 LTR: basal transcription (*Left*) and transcription in the presence of Tat-positive feedback (*Right*). (*C*) Reactivation of LTR Tax latency. Several Jurkat subclones stably transfected with HTLV-1-LTR-d2EGFP-2A Tax (Jurkat/LTRd2EGFP Tax cells) were established. All subclones had a similar latent phenotype and could be drastically reactivated by PMA/Ionomycin + JQ1 treatment. (*D*) Transient expression of Tax and d2EGFP in Jurkat/LTRd2EGFP Tax cells. White arrowheads indicate cells transiently expressing Tax. Cells were seeded in CytoCapture imaging dish (zell-kontakt GmbH) coated with Fibronectin (Corning).

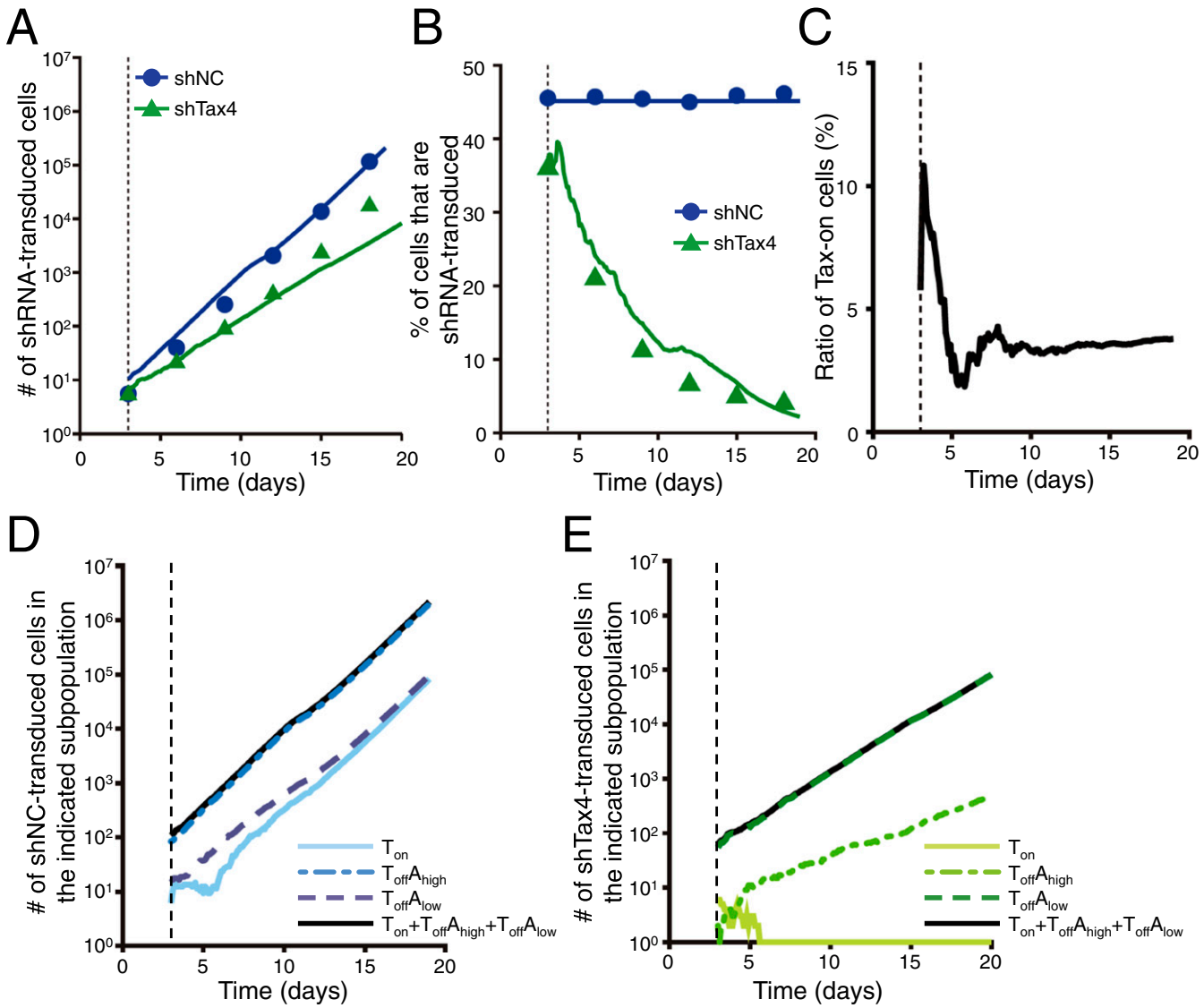

Fig. S6. An agent-based simulation using Tax period sampling from previously simulated values. The simulation in this figure resembles the simulation in Fig. 5, except that Tax period sampling is done from simulated values (i.e., the gray bars in Fig. S3*C*) and Tax interval sampling is from simulated values (i.e., Fig. S3*G*). (*A* and *B*) Time course of the number and fraction of shNC and shTax4 cells. (*C*) The simulated dynamics of the frequency of Tax-positive cells in the normal MT-1 cell population. (*D* and *E*) The simulated dynamics of subpopulations of cells transduced with shNC (*D*, blue lines) or shTax4 (*E*, green lines).

Table S1. Chemical reaction scheme and parameter values for stochastic simulation of the intracellular Tax expression model

Reactions	Description	Rate and value*
$5'\ LTR_{OFF} \leftrightarrow 5'\ LTR_{ON}$	Promoter toggling from active to inactive state	$k_{ON} = 3.0 \times 10^{-6}$,† $k_{OFF} = 1.0 \times 10^{-2}$‡
$5'\ LTR_{ON} \rightarrow 5'\ LTR_{ON} + mRNA$	Transcription of mRNA encoding Tax	$k_m = 0.1$‡
$mRNA \rightarrow mRNA + Tax$	Translation	$k_p = 10$‡
$5'\ LTR_{OFF} + Tax \leftrightarrow 5'\ LTR_{ON\text{-}Tax}$	Tax binding/unbinding to 5′ LTR	$k_{bind} = 2.5 \times 10^{-3}$,† $k_{unbind} = 1.8 \times 10^{-2}$†
$5'\ LTR_{ON\text{-}Tax} \rightarrow 5'\ LTR_{ON\text{-}Tax} + mRNA$	Transactivated rate of transcription	$k_a = 5$‡
$mRNA \rightarrow \varphi$	mRNA decay	$\delta_m = 1$‡
$Tax \rightarrow \varphi$	Tax decay	$\delta_p = 0.125$‡

*Time in simulation is in arbitrary units.
†These parameter values, which are specific to HTLV-1, are estimated from experimental data by fitting.
‡These parameter values are fixed as estimated in ref. 1.

1. Razooky BS, Pai A, Aull K, Rouzine IM, Weinberger LS (2015) A hardwired HIV latency program. *Cell* 160:990–1001.

Table S2. Parameter values for agent-based simulation of cell population dynamics under normal and Tax-KD conditions

Parameter	Description	Unit	Value
g_{on}	Growth rate of Tax-expressing cells	Day^{-1}	0.54†
g	Growth rate of Tax-negative cells with or without antiapoptotic gene expression	Day^{-1}	0.68†
p	Decay rate of antiapoptotic gene expression for $T_{off}A_{high}$ for shNC cells	Day^{-1}	0.02†
p^*	Decay rate of antiapoptotic gene expression for $T_{off}A_{high}$ for shTax4 cells	Day^{-1}	0.40†
δ	Apoptosis rate for $T_{off}A_{low}$ cells	Day^{-1}	0.25†

†These parameter values are estimated from experimental data by fitting.

Table S3. Primers used in the single-cell qPCR

	Preamplification primers		qPCR primers	
Gene	Forward	Reverse	Forward	Reverse
ACTB	CCTTCCAGCAGATGTGGATCAG	TCATCTTGTTTTCTGCGCAAGTTAG	AAGCAGGAGTATGACGAGTCC	CAAGAAAGGGTGTAACGCAACT
ATF3	GCTGTCTTCCTGTGTACCTCTA	AAATCCTGGAGTTGAGGCAAAG	CAGCAGCAGAGAACCATCAAG	CTGGTCCAAGACCCACTCTG
BCL2	GGATTGTGGCCTTCTTTGAGTT	CCAGCCTCCGTTATCCTGG	TGGGGTCATGTGTGTGGAGAG	GGTGCCGGTTCAGGTACTCA
BCL2A1	CGTCCAGAGTGCTACAAAATGT	CCGTCTTCAAACTCCTTTTCCA	GAAGTGGAAAAGAATCTGAAGTCATGC	TCACTTGGTTGAATAGTGTTCTGGC
BCL2L1	CCTAAGGCGGATTTGAATCTCTT	TATAATAGGGATGGGCTCAACCAG	CTCTCCCTTCAGAATCTTATCTTGG	ATTGTCCAAAACACCTGCTCAC
BCL3	CAGGATTTGCACAGAAGCACAT	GGAAATGGAAGATGTGGGTGG	CTCTTCTGAGCACAGATGTTCC	CATTCCGGACAGGGACTGG
BIRC5	GACCACCGCATCTCTACATTC	GCTCCTTGAAGCAGAAGAAACA	AAGAACTGGCCCTTCTTGGAG	AAGTCTGGCTCGTTCTCAGTG
CADM1	GAAGTACAGTATAAGCCTCAAGTGC	TTCATCATCGACTCTCACCCAA	CAGATGACTTATCCTCTACAAGGCT	GTTACCATCACAGGCTGGGG
CASP4	TGGGCTCTATCTTCATCACACA	TCATGGACAGTCGTTCTATGGT	GAAATATTCTTGGTGCTGCCAC	GCATTTGAGCTTTGGCCCTT
CASP8	CTTTGACCACGACCTTTGAAGA	CATGGGAGAGGATACAGCAGAT	TCATTTTGAGATCAAGCCCCAC	GTTACTGTGGTCCATGAGTTGG
CCL20	GTGCTTATCTAATTTGTGCCTCACT	TAGCTAAACACAGAAAACCTACAGC	CTAATTTGTGCCTCACTGGACT	TGTGATGCTTAAACAAAGCAAACT
CCL22	CTTCTACTGGACCTCAGACTCC	GGTCATCAGAGTAGGCTCTTCA	CGTGGTGTTGCTAACCTTCAG	TTGGCTCAGCTTATTGAGAATCA
CCL3	CTGCAACCAGTTCTCTGCATC	TTAGGAAGATGACACCGGGC	CTTGCTGCTGACACGCCG	GCTGCTCGTCTCAAAGTAGTCA
CCND2	GGAAGTTGAAGTGGAACCTGG	CAAACTTAAAGTCGGTGGCACA	TGACTTCATTGAGCACATCTTGC	AGAGCAATGAAGGTCTGAGCAT
CCR10	CTAGGGCTGCGAATCTAGAGG	GGGTTGCATCTCATTTCCATGT	GGTCGTGGGAAAGGGGAGTA	TTTAATGTGGCAAGGCACAGA
CCR4	AAAGCAAGCTGCTTCTGGTTG	TGCAAGGCTTGGGGATACTTT	GCCCAGACCTGCCTTGAG	TTGCTGTATATGCTTTCATCGAGGG
CCR6	GATACAGTCAACAAGCCTGACC	CAACCTGAGCTGCTTTATCCAA	AAATGGAGGTGGAAAGACAAGC	AATTGTCACCAACACCTGTTCT
CCR9	GGAAGTTCCAGACCTTCATGTG	TTTCTCCCTCCAAGTATGTGCT	GGTCAACAGCATGTACAAGATGAAC	GGCAATGGCAATGTACCTGT
CD48	ATGGAAGATCAAGCTGCAAGTG	TTTTGTCCCCATACCAGGTGTA	GTACCCAAGCCTGTCATCAAAA	TTTACAGACTCGCCAGGTATCA
CD55	CCCTAATCCGGGAGAAATACGA	GGACAGAGCTGCCTGAAATAAG	AATGGTCAGATTGATGTACCAGG	AATAATTTGTACCCTGTGTTACATGAGAAG
CD69	GAGCTCCAGCAAAGACTTTCAC	GGACTGGTGGCATCATTTTCTT	GACTTGACCTGAGATTAACTAGGGA	TCCACTCTCCGGATGCAAAG
CD82	GATGGGCTCAGCCTGTATCAA	GGAGGTTTGCAGGACAGAGAT	GTCACCAAATACTTTCTCTTCCTCTTC	GAAACTGCTCTTGTCGGCCA
CD99	TTAATCTTGCGATGTGCTTTGC	AATAATGGCCAGCCTTTCACAT	GCTGGGCGGATGATGTTTACTA	GGGCCTTGGAGAATGGGG
CDC25B	CTGGACAAGAGAGTCATCCTCA	TAGCCGCCTTTCAGGATATACA	TGTGAATTCTCATCTGAGCGTG	GTAGTAGAGGCTGGGGTAGTC
CDKN1A	ACCAGCATGACAGATTTCTACC	CACACAAACTGAGACTAAGGCA	CGGCTGATCTTCTCCAAGAGG	GAAGATGTAGAGCGGGCCTTT
CFLAR	CCCCTAGGAATCTGCCTGATAA	TACAGGCAAATTGGCCAAGAAT	ATTGGCAATGAGACAGAGCTTC	TGGGATATACCATGCATACTGAGA
COL1A1	AGACATGTTCAGCTTTGTGGAC	GTACCTGAGGCCGTTCTGTA	GGCTCCTGCTCCTCTTAGC	AGGTGATTGGTGGGATGTCTT
CREB3	GGCTAGTACTGACAGATGAGGA	GGCTCTCTTGAGCAGATCTTTTA	AGAGTCTATTGGAGAAGGAGGG	CGCACACGTTTCAGAATTTGTT
CXCL10	TGTCCACGTGTTGAGATCATTG	GATTTTGCTCCCCTCTGGTTTT	GGTGAGAAGAGATGTCTGAATCC	GAGATCTTTTAGACCTTTCCTTGCT
CXCL11	TGGGGTAAAAGCAGTGAAAGTG	ATAAGCCTTGCTTGCTTCGATT	AGCCTCCATAATGTACCCAAGT	GGATTTAGGCATCGTTGTCCTTT
CXCL8	AAACTTTCAGAGACAGCAGAGC	CAGAGCTGCAGAAATCAGGAAG	ACAAGCTTCTAGGACAAGAGCC	GCCAGCTTGGAAGTCATGTTTA
DUSP1	GAAATCCTGCCCTTTCTGTACC	AGGGATGCTCTTGTACTGGTAG	CAGTGCGTATCACGCTTCC	CCCTCAAAATGGTTGGGACAAT
DUSP2	GATCTTGCCCTACCTGTTCCT	TCCACAGGGATACTCTTGTAGC	CTGCAGTCACTCGTCAGACC	GAAAAGGCCCTCAAAGTGGTTG
EGR1	TAGGTCAGATGGAGGTTCTCAG	AGAACTTGGACATGGCTGTTTC	CAAGTCCTCCCTCTCTACTGGA	GCAGCTGAAGTCAAAGGGAATA
FZD6	CTTGGGTCTCTGATCATTGTCG	TTTTGCTTCCAACCCAGAAGAC	CCCATGTCCTTATCAGGCAAAA	TGCCAACAATTAATGTCATCAGGT
GADD45B	GAGTCGGCCAAGTTGATGAATG	ACGATGTTGATGTCGTTGTCAC	CTGCCTCTTGGCCATTGACGA	AGCAGAAGGACTGGATGAGCG
HIF1A	TACAGGATGCTTGCCAAAAGAG	GGAGAAAATCAAGTCGTGCTGA	CTGGGTTGAAACTCAAGCAACT	ACCACTCACAACGTAATTCACA
HIGD1A	ACAGGTGTTTCCCTTCCTTCAT	AGTATTTCCCCTGCTCTTCAGT	GGAAGATCAGGGATCAAAACTCA	CAACAATTGCTGCAAAACCCG
ICAM1	ATGTGCAAGAAGATAGCCAACC	GGTAAGGTTCTTGCCCACTG	GCTATTCAAACTGCCCTGATGG	GGAGGGGTGCCAGTTCCA
ID2	TCAAATGACAGCAAAGCACTGT	CCATTCAACTTGTCCTCCTTGT	GTGGCTGAATAAGCGGTGTTC	AAGTTCAGCACTTAAAAGATTCCGTG
IFIT2	TCAGCATTTATTGGTGGCAGAA	ATGGCATTTTAGTTGCCGTAGG	GGAAGATTTCTGAAGAGTGCAGC	CTGCTCTCCAAGGAATTCTTATTGT
IFIT3	GGCAGTATTTTCCTGTCAGCAT	AGGCTTCTGATGCTCTGTTTTC	TGAGCTTGAGGATGGTAGTGAG	TCTGTCTCAGTTCAGTTGCTCT
IKZF1	ATATTGGAGACCGGAGGGTAAC	TTACAGAAGGGATATGGGGCAA	GTTGGCCTGTTGATTACAGCTA	TGAGATCCAGGCTTTCCACAT
IL10RA	CTCCTAACCTCTGGAGAAGTGG	AGAAGATGATGACGTTGGTCAC	GAGTTCTGTGTCCAGGTGAAAC	GTGAAATACTGCCTGGTGAGG
IL13	TCATTGCTCTCACTTGCCTTG	GTTGATGCTCCATACCATGCTG	CCTGTGCCTCCCTCTACAGC	CATTGCAGAGCGGAGCCTTC
IL15	GAAGTGCTTTCTCTTGGAGTTACA	TCCTCACATTCTTTGCATCCAG	ATTTCACTTGAGTCCGGAGATG	GAAGACAAACTGTTGTTTGCTAGG
IL23A	TGATGTTCCCCATATCCAGTGT	AGAAGGCTCCCCTGTGAAAATA	CCCAAGGACTCAGGGACAAC	TCCGATCCTAGCAGCTTCTCAT
IL2RA	GGAAGACAAGGTGGACCCAG	TGAAAATCTGTTGTTGTGACGAGG	CAGCTCATATGCACAGGTGAAA	CAGGAAGTCTCACTCTCAGGAC
IMMT	GCTCGGGATGACTTTAAACGAG	TCAATACGACGATGTGCATGAG	AGCTGGACAGTATTACTCCAGAA	CATCAGTAGAGAGCTTGTCAGC
INSIG1	ACTGCATTAAACGTGTGGTGTT	ACAAGGCTCAGATTGGTTTTCA	GTGAGCACAATGTATTCATTTAATGGC	TGCACTTGAAGTTTAAGACCCA
JUNB	GCACTAAAATGGAACAGCCCTT	CTTTGAGACTCCGGTAGGGG	TACCACGACGACTCATACACAG	GCTCGGTTTCAGGAGTTTGTAG
LSP1	TATTGTGGCTGGAGACATGAGC	TCCACAAGCACCTTCTCATACT	AAGAAAAGCCTCTGGGAGCAGAA	CGGTGGCCACAAACTTATACCT
LY75	AAGAGTTGTCTGCAAAGTGCC	GAACTGATGAGAAACCCGCC	GGCCCTGATTACACAGCAATAG	GAAGAGGAACCAAATCAGTCCG
MAP3K14	GCAGCTGGAAATAGAATTATTCCTC	GAGCTTTGAGAGGCCTTTGATG	CCTGTCCCAGCCATTTTCTCT	GGTTCTTCTCACTGTCATCCGA
MT1X	CCACGCTTTTCATCTGTCCC	GTGCATTTGCACTCTTTGCATT	CTGCGTGTTTTCCTCTTGATCG	CAGGCACAGGAGCCAACAG
MT2A	AATGCACCTCCTGCAAGAAAAG	TGGAAGTCGCGTTCTTTACATC	TGGGCTGTGCCAAGTGTG	GGGCTGTCCCAGCATCAG
MYD88	CAATTCCTGGAGATGCCAACTT	GTCTCAGCTGGTCCTGTTCTAT	CAGCAGCTGGACATCACATTTC	GGCTGATAATCCAGCAAGTGG
NFKB1	CCGTGTAAACCAAAGCCCTAAA	GAACCAAGAAAGGAAGCCAAGT	ATTCCACTGCGTTGTCCAC	AAATCGAGAATGATTCAGGCGG
NFKB2	TGTTGCATATGCCTGACTTTGA	CTAGATGCAAGGCTGTTCGTC	CTGTATCCAGTACACCTGGCGG	CTCCACTTCAGCCCCACTGTC
NFKBIA	AATGCTCAGGAGCCCTGTAA	AGGTGAGCTGGTAGGGAGAAT	CCTTCACCTCGCAGTGGAC	CCCTGGTAGGTAACTCTGTTGA
NR4A1	ATAGCGCCGTGCTGTAAATAAG	GAAGGAGGGTAGGAAGAGAGAG	CAGGAAGAAAGAGCTTGAGGTG	CAGCAGGAGGCTGGAAAGG
NR4A2	GAATGAATGAAGAGAGACGCGG	TTACAGGCGTTTTCGAGGAAAT	CCTAAGGAGGAGATTGGACAGG	AGGTGGACAGTGTCGTAATTCA
PHF13	ATGATGAGGACATCATGGTGGA	ATTTCCGGATTTTCGCACAGG	CTCAGATGACGATTCCTGGGAC	TGGCACTCATTACACTCGATCA
PKMYT1	CCTCACCATCCTGGAAGTGG	CTCCAGCATCATGACAAGGAC	CATGCAACATGGAGCTGCCC	GAAGACAGACCGGCAGTGAA
PPP1R21	TGCGTTAAGAGCCAGGAATCTA	ACACAGAACTGTAGTTTGTCCG	TGACAGCTGTGTTTGAGAAGC	AAGGAGTCCATCTGGCTCTGTA
PRKACB	CTGGAGATACCAGCAACTTTGA	TCTCTCAACAGAGTGCAAACAC	TGACTATGAAGAAGAAGATATCCGTG	GTCATCTTGTTCCTCTTTAAAATTCACC
PYCARD	CCTAAGGGAGTCCCAGTCCTA	CAAGCTGGCTTTTCGTATATTGTG	CTGGTGGAGGACCTGGAG	TCAGGATGATTTGGTGGGATTG
RELA	GCTTGTAGGAAAGGACTGCC	TTGTTGTTGGTCTGGATGCG	GGATGGCTTCTATGAGGCTGAG	CCGCTTCTTCACACACTGGATT
RGS1	TGCAATGGTCTCAATCTCTGGA	GCTTTACAGGGCAAAAGATCAGA	TGCCAACCAAACTGGTCAAAAT	TTATAGTCTTCACAAGCCAGCC
SELPLG	CTCTAACATCTCCCATGGCTCT	AATGTCCACTTCCTGTTTGGTG	CTTCTCCTGGTCACTGGAGTC	CATGGCAACCAAAAGACAATGG
SMAD7	GCTTTCAGATTCCCAACTTCTTCT	CCATTCCCCTGAGGTAGATCAT	GGATCGGTCACACTGGTGC	AGAAGATATCCAGAGAGGGCTCC
SMIM4	TCCAGTGCTTAGTTCCGTCATA	ATCGTTCCTCCCAGGACAAAA	GGTCGAGCATGTTCACCAG	AGGAACCGGTAGATGCCAAATC
STAT1	GACCGCACCTTCAGTCTTTTC	GCAATTTCACCAACAGTCTCAAC	TCATTCAGAGCTCGTTTGTGG	AGTGAACTGGACCCCTGTCT
STAT3	CACTACTAAAGTCAGGTTGCTGG	CATCACTTTTGTGTTTGTGCCC	TTCCCTGAGTTGAATTATCAGCTT	AATGTTAAATTTCCGGGATCCTCT
STAT4	CTAATGCTTGGGCATCCATCAT	TCTGAGTTAAGACCACGACCAA	CAACGATTCCCAGAACTTGGTT	ATGAAAACTGCCAGCTCATCAC
STAT5A	CACAGAACCCTGACCATGTACT	AGAGGTGAAAAGACCGGCAG	GGATGGAGAATTCGACCTGGAT	CGGGAGTCAAGACTGTCCATT
STAT5B	CTACGTGTTTCCTGATCGGC	AGATGCGTTCACAAACTCAGG	TACTCCAAATACTACACACCAGTTC	GACCACTTGCTTGATCTGTGG
THEMIS2	AGAAGGTGGTCTGTGAGAACC	TGCTTGGAGCTCTGAGTTGT	CGAAGACCAGCCAGACCAT	CTCCTCCAGGGTTTCATAGCTC
TNFAIP3	GACACAGACTTGGTACTGAGGA	TCCAGTTCCGAGTATCATAGCA	TTCAGCACGCTCAAGGAAAC	AAGCCCCGTTTCAACAAATTCC
TNFRSF1B	CATGCCGGCTCAGAGAATACTA	AGTTCCAGAGCTGGGTGTATG	TGCAGCAAATGCTCGCCG	CTGTCCTCACAGGAGTCACAC
TNFRSF9	CAGGATGCAGCATGTGTGAA	GACTTTCCATCCAAAGAACAGTTTG	CAGGATTGTAAACAAGGTCAAGAAC	GACAGATGCCACGTTTCTGAT
TNFSF10	GGCATTCATTCCTGAGCAACTT	TGGACCATTTGTTTGTCGTTCT	CACTTGAGGAATGGTGAACTGG	TTTCCTCCTGAAATCGAAAGTATGT
TNFSF4	GTCTGTCAACTCCTTGATGGTG	AGGACACAGAATTCACCAGGAT	GCCTCTCTGACTTACAAAGACAA	AAGAATCAGTTCTCCGCCATTC
TNIP1	CTGGCCAAGTCCAAGATTGAAA	GCTGGATCTCCTTTTCCTGGTA	TGGAGGAGACCGACAAGGAG	CTCACGCTGTCGGGTGAGT
TP53	GCTCAGATAGCGATGGTCTGG	GTACAGTCAGAGCCAACCTCAG	CTCCTCAGCATCTTATCCGAGT	ATAGGGCACCACCACACTATG
TRAF1	CACTTTCCTGTGGAAGATCACC	TGCCATCTCCATTCAGGTACAG	AATGTCACCAGGCGGTGC	CATACTTGGCAGTGTAGAAGGC
UBE2C	ATAAGCTCTCGCTAGAGTTCCC	ATCATACAGGGCAGACCACTTT	CAGTGGCTACCCTTACAATGC	ATGTCCAGGCATATGTTACCCT
WIPI1	ATGGATTCACAATTCCTCTGCG	AGGTAGTTGGTAGCAGCCATAA	CCGAGACGGTACACATCTTCAA	ACATCTTTCCCATGTAGCCACT
tax	GATCCCAAAGAAAAAGACCACCA	CTCCAAACACGTAGACTGGGTA	GATCCCAAAGAAAAAGACCACCA	CTCCAAACACGTAGACTGGGTA
hbz	TAAACTTACCTAGACGGCGGAC	ACCAATTCCTCCACCAGCAG	CAGTTCAGGAGGCACCACAG	ACAGGCAAGCATCGAAACAG
Spike1	GTATTTGATTACCGGCAACGGA	ACCGTCGTCATTGAAGATATGC	GTGCATTCTCTGGAAGGTGAAC	CTCGGGTATCCCATTGCTGAT
Spike4	ATGCGTAGATAACATTCAGGCG	GTGGTGAAATTCGATCCTACCG	AAGAGCTGTACACCGTAGTGG	CCACATCTTTGGCAGCGAAT
Spike7	GAGAAAGGTAATGACCTGGTGC	TTTGGGTATTGAAGATCAGGCG	TCCCATATGCTGGAAGTCTGC	GATCGTCCTTACCACCAATACC

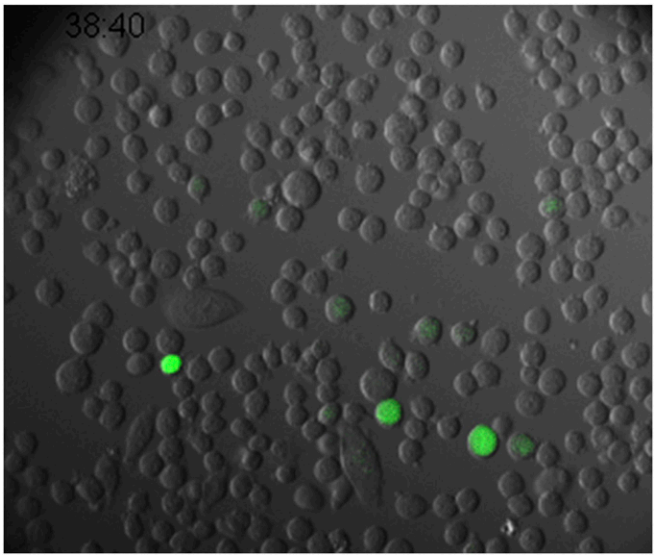

Movie S1. Time-lapse imaging of MT1GFP cells. Tax is transiently expressed in a small subpopulation of MT1GFP.

Movie S1